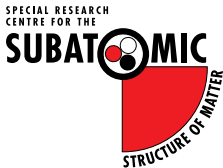


# New insights into the quark model from lattice QCD

Derek Leinweber

In collaboration with: Curtis Abell, Liam Hockley, Waseem Kamleh,  
Yan Li, Zhan-Wei Liu, Finn Stokes, Tony Thomas, Jia-Jun Wu



# The spectrum of a simple quark model: $N$ and $\Lambda$ baryons

$N(1/2+)$  —————  $2h\omega$   
~2.0 GeV

$\Lambda(1/2-)$  —————  
 $N(1/2-)$  —————  $1h\omega$   
~1.5 GeV

$\Lambda(1/2+)$  —————  
 $N(1/2+)$  —————  $0h\omega$   
~1 GeV Quark Model

# The challenge of experiment

$N(1/2+)$  —————  $2h\omega$   
~2.0 GeV



$\Lambda(1/2-)$  —————  
 $N(1/2-)$  —————  $1h\omega$   
~1.5 GeV

$\Lambda^*(1670)$  —————  
 $N^*(1535)$  —————  
 $N^*(1440)$  —————  
 $\Lambda^*(1405)$  —————

$\Lambda(1/2+)$  —————  
 $N(1/2+)$  —————  $0h\omega$   
~1 GeV    Quark Model

$\Lambda(1115)$  —————  
 $N(940)$  —————  
Experiment

# Prologue

---

- The idea of dressing quark-model states in a coupled-channel analysis to describe scattering data has been around for decades.

# Prologue

---

- The idea of dressing quark-model states in a coupled-channel analysis to describe scattering data has been around for decades.
- What's new are formalisms able to bring these descriptions to the finite-volume of lattice QCD.

# Prologue

---

- The idea of dressing quark-model states in a coupled-channel analysis to describe scattering data has been around for decades.
- What's new are formalisms able to bring these descriptions to the finite-volume of lattice QCD.
- Lattice QCD calculations of the excitation spectrum provide new constraints.

# Prologue

---

- The idea of dressing quark-model states in a coupled-channel analysis to describe scattering data has been around for decades.
- What's new are formalisms able to bring these descriptions to the finite-volume of lattice QCD.
- Lattice QCD calculations of the excitation spectrum provide new constraints.
- It's time to reconsider our early notions about the quark-model and its excitation spectrum.

# Outline

---

- Hamiltonian Effective Field Theory (HEFT)
  - Coupled-channel analysis technique aimed at resonance physics.
  - Incorporates the Lüscher formalism.
  - Connects scattering observables to the finite-volume spectrum of lattice QCD.



# Outline

---

- Hamiltonian Effective Field Theory (HEFT)
  - Coupled-channel analysis technique aimed at resonance physics.
  - Incorporates the Lüscher formalism.
  - Connects scattering observables to the finite-volume spectrum of lattice QCD.
- $\Delta$  Resonance: introduce HEFT and illustrate the constraints provided by Lüscher.

# Outline

---

- Hamiltonian Effective Field Theory (HEFT)
  - Coupled-channel analysis technique aimed at resonance physics.
  - Incorporates the Lüscher formalism.
  - Connects scattering observables to the finite-volume spectrum of lattice QCD.
- $\Delta$  Resonance: introduce HEFT and illustrate the constraints provided by Lüscher.
- $N^*(1535)$  and  $N^*(1650)$  Resonances: novel two quark-model basis-state analysis.

# Outline

- Hamiltonian Effective Field Theory (HEFT)
  - Coupled-channel analysis technique aimed at resonance physics.
  - Incorporates the Lüscher formalism.
  - Connects scattering observables to the finite-volume spectrum of lattice QCD.
- $\Delta$  Resonance: introduce HEFT and illustrate the constraints provided by Lüscher.
- $N^*(1535)$  and  $N^*(1650)$  Resonances: novel two quark-model basis-state analysis.
- $\Lambda(1405)$  Resonance: evidence of a molecular  $\bar{K}N$  component

# Outline

- Hamiltonian Effective Field Theory (HEFT)
  - Coupled-channel analysis technique aimed at resonance physics.
  - Incorporates the Lüscher formalism.
  - Connects scattering observables to the finite-volume spectrum of lattice QCD.
- $\Delta$  Resonance: introduce HEFT and illustrate the constraints provided by Lüscher.
- $N^*(1535)$  and  $N^*(1650)$  Resonances: novel two quark-model basis-state analysis.
- $\Lambda(1405)$  Resonance: evidence of a molecular  $\bar{K}N$  component
- Roper  $N(1440)$  Resonance:
  - Lattice QCD results constrain the HEFT description of experimental data.

# Outline

- Hamiltonian Effective Field Theory (HEFT)
  - Coupled-channel analysis technique aimed at resonance physics.
  - Incorporates the Lüscher formalism.
  - Connects scattering observables to the finite-volume spectrum of lattice QCD.
- $\Delta$  Resonance: introduce HEFT and illustrate the constraints provided by Lüscher.
- $N^*(1535)$  and  $N^*(1650)$  Resonances: novel two quark-model basis-state analysis.
- $\Lambda(1405)$  Resonance: evidence of a molecular  $\bar{K}N$  component
- Roper  $N(1440)$  Resonance:
  - Lattice QCD results constrain the HEFT description of experimental data.
- Conclusions

# Hamiltonian Effective Field Theory (HEFT)

J. M. M. Hall, *et al.* [CSSM], Phys. Rev. D **87** (2013) 094510 [arXiv:1303.4157 [hep-lat]]

C. D. Abell, DBL, A. W. Thomas, J. J. Wu, Phys. Rev. D **106** (2022) 034506 [arXiv:2110.14113 [hep-lat]]

- An extension of chiral effective field theory incorporating the Lüscher formalism
  - Linking the energy levels observed in finite volume to scattering observables.

# Hamiltonian Effective Field Theory (HEFT)

J. M. M. Hall, *et al.* [CSSM], Phys. Rev. D **87** (2013) 094510 [arXiv:1303.4157 [hep-lat]]

C. D. Abell, DBL, A. W. Thomas, J. J. Wu, Phys. Rev. D **106** (2022) 034506 [arXiv:2110.14113 [hep-lat]]

- An extension of chiral effective field theory incorporating the Lüscher formalism
  - Linking the energy levels observed in finite volume to scattering observables.
- In the light quark-mass regime, in the perturbative limit,
  - HEFT reproduces the finite-volume expansion of chiral perturbation theory.

# Hamiltonian Effective Field Theory (HEFT)

J. M. M. Hall, *et al.* [CSSM], Phys. Rev. D **87** (2013) 094510 [arXiv:1303.4157 [hep-lat]]

C. D. Abell, DBL, A. W. Thomas, J. J. Wu, Phys. Rev. D **106** (2022) 034506 [arXiv:2110.14113 [hep-lat]]

- An extension of chiral effective field theory incorporating the Lüscher formalism
  - Linking the energy levels observed in finite volume to scattering observables.
- In the light quark-mass regime, in the perturbative limit,
  - HEFT reproduces the finite-volume expansion of chiral perturbation theory.
- Fitting resonance phase-shift data and inelasticities,
  - Predictions of the finite-volume spectrum are made.



# Hamiltonian Effective Field Theory (HEFT)

J. M. M. Hall, *et al.* [CSSM], Phys. Rev. D **87** (2013) 094510 [arXiv:1303.4157 [hep-lat]]

C. D. Abell, DBL, A. W. Thomas, J. J. Wu, Phys. Rev. D **106** (2022) 034506 [arXiv:2110.14113 [hep-lat]]

- An extension of chiral effective field theory incorporating the Lüscher formalism
  - Linking the energy levels observed in finite volume to scattering observables.
- In the light quark-mass regime, in the perturbative limit,
  - HEFT reproduces the finite-volume expansion of chiral perturbation theory.
- Fitting resonance phase-shift data and inelasticities,
  - Predictions of the finite-volume spectrum are made.
- The eigenvectors of the Hamiltonian provide insight into the composition of the energy eigenstates.
  - Insight is similar to that provided by correlation-matrix eigenvectors in Lattice QCD.

# Infinite Volume Model

- The rest-frame Hamiltonian has the form  $H = H_0 + H_I$ , with

$$H_0 = \sum_{B_0} |B_0\rangle m_{B_0} \langle B_0| + \sum_{\alpha} \int d^3k |\alpha(\mathbf{k})\rangle \omega_{\alpha}(\mathbf{k}) \langle \alpha(\mathbf{k})|,$$

# Infinite Volume Model

- The rest-frame Hamiltonian has the form  $H = H_0 + H_I$ , with

$$H_0 = \sum_{B_0} |B_0\rangle m_{B_0} \langle B_0| + \sum_{\alpha} \int d^3k |\alpha(\mathbf{k})\rangle \omega_{\alpha}(\mathbf{k}) \langle \alpha(\mathbf{k})|,$$

- $|B_0\rangle$  denotes a quark-model-like basis state with bare mass  $m_{B_0}$ .

# Infinite Volume Model

- The rest-frame Hamiltonian has the form  $H = H_0 + H_I$ , with

$$H_0 = \sum_{B_0} |B_0\rangle m_{B_0} \langle B_0| + \sum_{\alpha} \int d^3k |\alpha(\mathbf{k})\rangle \omega_{\alpha}(\mathbf{k}) \langle \alpha(\mathbf{k})|,$$

- $|B_0\rangle$  denotes a quark-model-like basis state with bare mass  $m_{B_0}$ .
- $|\alpha(\mathbf{k})\rangle$  designates a two-particle non-interacting basis-state channel with energy

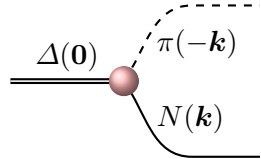
$$\omega_{\alpha}(\mathbf{k}) = \omega_{\alpha_M}(\mathbf{k}) + \omega_{\alpha_B}(\mathbf{k}) = \sqrt{\mathbf{k}^2 + m_{\alpha_M}^2} + \sqrt{\mathbf{k}^2 + m_{\alpha_B}^2},$$

for  $M = \text{Meson}$ ,  $B = \text{Baryon}$ .

# Infinite Volume Model

- The interaction Hamiltonian includes two parts,  $H_I = g + v$ .
- $1 \rightarrow 2$  particle vertex

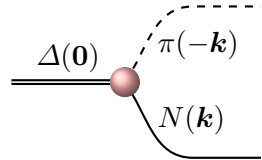
$$g = \sum_{\alpha, B_0} \int d^3k \left\{ |\alpha(\mathbf{k})\rangle G_{\alpha, B_0}^\dagger(k) \langle B_0| + h.c. \right\} ,$$



# Infinite Volume Model

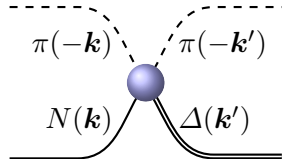
- The interaction Hamiltonian includes two parts,  $H_I = g + v$ .
- $1 \rightarrow 2$  particle vertex

$$g = \sum_{\alpha, B_0} \int d^3k \left\{ |\alpha(\mathbf{k})\rangle G_{\alpha, B_0}^\dagger(k) \langle B_0| + h.c. \right\},$$



- $2 \rightarrow 2$  particle vertex

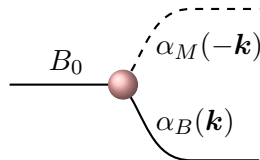
$$v = \sum_{\alpha, \beta} \int d^3k d^3k' |\alpha(\mathbf{k})\rangle V_{\alpha, \beta}^S(k, k') \langle \beta(\mathbf{k}')|.$$



## S-wave vertex interactions

- S*-wave vertex interactions between the one baryon and two-particle meson-baryon channels for e.g.  $N^*(1535)$  or  $\Lambda^*(1405)$  cases take the form

$$G_{\alpha, B_0}(k) = g_{B_0\alpha} \frac{\sqrt{3}}{2\pi f_\pi} \sqrt{\omega_{\alpha_M}(k)} u(k, \Lambda),$$



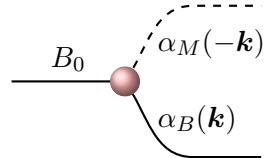
with regulator

$$u(k, \Lambda) = \left( 1 + \frac{k^2}{\Lambda^2} \right)^{-2}, \quad \text{and fixed } \Lambda \sim 0.8 \rightarrow 1.0 \text{ GeV}.$$

## $P$ -wave and higher vertex interactions

- $P$ -wave and higher vertex interactions for the  $\Delta(1232)$  or  $N^*(1440)$  take the form

$$G_{\alpha, B_0}(k) = g_{B_0\alpha} \frac{1}{4\pi^2} \left( \frac{k}{f_\pi} \right)^{l_\alpha} \frac{u(k, \Lambda)}{\sqrt{\omega_{\alpha_M}(k)}},$$



where  $l_\alpha$  is the orbital angular momentum in channel  $\alpha$ .



## Two-to-two particle interactions

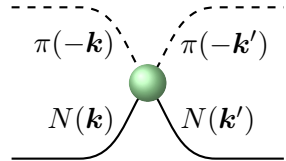
---

- For the direct two-to-two particle interaction, we introduce separable potentials.

## Two-to-two particle interactions

- For the direct two-to-two particle interaction, we introduce separable potentials.
- For the  $S_{11}$   $\pi N$  channel

$$V_{\pi N, \pi N}^S(k, k') = v_{\pi N, \pi N} \frac{3}{4\pi^2 f_\pi^2} \tilde{u}_{\pi N}(k, \Lambda) \tilde{u}_{\pi N}(k', \Lambda)$$



where the scattering potential gains a low energy enhancement via

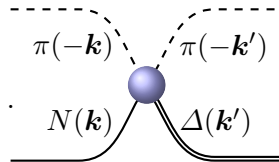
$$\tilde{u}_{\pi N}(k, \Lambda) = u(k, \Lambda) \frac{m_\pi^{\text{phys}} + \omega_\pi(k)}{\omega_\pi(k)}$$

and  $u(k, \Lambda)$  takes the dipole form.

## Two-to-two particle interactions

- For  $P$ -wave scattering in the  $\Delta(1232)$  or  $N^*(1440)$  channels

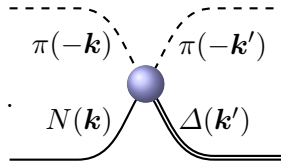
$$V_{\alpha,\beta}^S(k, k') = v_{\alpha,\beta} \frac{1}{4\pi^2 f_\pi^2} \frac{k}{\omega_{\alpha_M}(k)} \frac{k'}{\omega_{\beta_M}(k')} u(k, \Lambda) u(k', \Lambda).$$



## Two-to-two particle interactions

- For  $P$ -wave scattering in the  $\Delta(1232)$  or  $N^*(1440)$  channels

$$V_{\alpha,\beta}^S(k, k') = v_{\alpha,\beta} \frac{1}{4\pi^2 f_\pi^2} \frac{k}{\omega_{\alpha_M}(k)} \frac{k'}{\omega_{\beta_M}(k')} u(k, \Lambda) u(k', \Lambda).$$



- For the  $\Lambda^*(1405)$ , the Weinberg-Tomozawa term is considered

$$V_{\alpha,\beta}^S(k, k') = g_{\alpha,\beta}^{\Lambda^*} \frac{[\omega_{\alpha_M}(k) + \omega_{\beta_M}(k')] u(k, \Lambda) u(k', \Lambda)}{16 \pi^2 f_\pi^2 \sqrt{\omega_{\alpha_M}(k) \omega_{\beta_M}(k')}},$$

## Infinite-Volume scattering amplitude

- The  $T$ -matrices for two particle scattering are obtained by solving the coupled-channel integral equations

$$T_{\alpha,\beta}(k, k'; E) = \tilde{V}_{\alpha,\beta}(k, k'; E) + \sum_{\gamma} \int q^2 dq \frac{\tilde{V}_{\alpha,\gamma}(k, q; E) T_{\gamma,\beta}(q, k'; E)}{E - \omega_{\gamma}(q) + i\epsilon}.$$

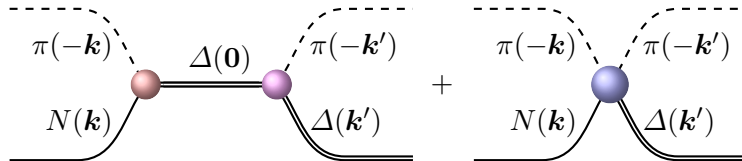
# Infinite-Volume scattering amplitude

- The  $T$ -matrices for two particle scattering are obtained by solving the coupled-channel integral equations

$$T_{\alpha,\beta}(k, k'; E) = \tilde{V}_{\alpha,\beta}(k, k'; E) + \sum_{\gamma} \int q^2 dq \frac{\tilde{V}_{\alpha,\gamma}(k, q; E) T_{\gamma,\beta}(q, k'; E)}{E - \omega_{\gamma}(q) + i\epsilon}.$$

- The coupled-channel potential is readily calculated from the interaction Hamiltonian

$$\tilde{V}_{\alpha,\beta}(k, k') = \sum_{B_0} \frac{G_{\alpha,B_0}^{\dagger}(k) G_{\beta,B_0}(k')}{E - m_{B_0}} + V_{\alpha,\beta}^S(k, k'),$$



# Infinite-Volume scattering matrix

- The S-matrix is related to the  $T$ -matrix by

$$S_{\alpha,\beta}(E) = 1 - 2i \sqrt{\rho_{\alpha}(E) \rho_{\beta}(E)} T_{\alpha,\beta}(k_{\alpha \text{ cm}}, k_{\beta \text{ cm}}; E),$$

with

$$\rho_{\alpha}(E) = \pi \frac{\omega_{\alpha_M}(k_{\alpha \text{ cm}}) \omega_{\alpha_B}(k_{\alpha \text{ cm}})}{E} k_{\alpha \text{ cm}},$$

and  $k_{\alpha \text{ cm}}$  satisfies the on-shell condition

$$\omega_{\alpha_M}(k_{\alpha \text{ cm}}) + \omega_{\alpha_B}(k_{\alpha \text{ cm}}) = E.$$

# Infinite-Volume scattering matrix

- The S-matrix is related to the  $T$ -matrix by

$$S_{\alpha,\beta}(E) = 1 - 2i \sqrt{\rho_{\alpha}(E) \rho_{\beta}(E)} T_{\alpha,\beta}(k_{\alpha \text{ cm}}, k_{\beta \text{ cm}}; E),$$

with

$$\rho_{\alpha}(E) = \pi \frac{\omega_{\alpha M}(k_{\alpha \text{ cm}}) \omega_{\alpha B}(k_{\alpha \text{ cm}})}{E} k_{\alpha \text{ cm}},$$

and  $k_{\alpha \text{ cm}}$  satisfies the on-shell condition

$$\omega_{\alpha M}(k_{\alpha \text{ cm}}) + \omega_{\alpha B}(k_{\alpha \text{ cm}}) = E.$$

- The cross section  $\sigma_{\alpha,\beta}$  for the process  $\alpha \rightarrow \beta$  is

$$\sigma_{\alpha,\beta} = \frac{4\pi^3 k_{\alpha \text{ cm}} \omega_{\alpha M}(k_{\alpha \text{ cm}}) \omega_{\alpha B}(k_{\alpha \text{ cm}}) \omega_{\beta M}(k_{\alpha \text{ cm}}) \omega_{\beta B}(k_{\alpha \text{ cm}})}{E^2 k_{\beta \text{ cm}}} |T_{\alpha,\beta}(k_{\alpha \text{ cm}}, k_{\beta \text{ cm}}; E)|^2.$$



## $\pi N$ phase shift and inelasticity

- The S-matrix is related to the  $T$ -matrix by

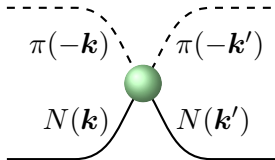
$$\begin{aligned}
 S_{\pi N, \pi N}(E) &= 1 - 2i\pi \frac{\omega_{\pi}(k_{\text{cm}}) \omega_N(k_{\text{cm}})}{E} k_{\text{cm}} T_{\pi N, \pi N}(k_{\text{cm}}, k_{\text{cm}}; E), \\
 &= \eta(E) e^{2i\delta(E)}.
 \end{aligned}$$

## $\pi N$ phase shift and inelasticity

- The S-matrix is related to the  $T$ -matrix by

$$\begin{aligned} S_{\pi N, \pi N}(E) &= 1 - 2i\pi \frac{\omega_{\pi}(k_{\text{cm}}) \omega_N(k_{\text{cm}})}{E} k_{\text{cm}} T_{\pi N, \pi N}(k_{\text{cm}}, k_{\text{cm}}; E), \\ &= \eta(E) e^{2i\delta(E)}. \end{aligned}$$

- In solving for the energy eigenstates...

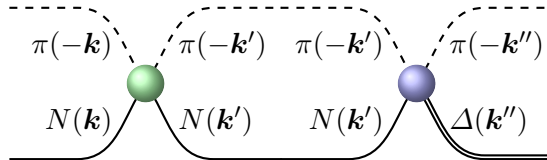


## $\pi N$ phase shift and inelasticity

- The S-matrix is related to the  $T$ -matrix by

$$\begin{aligned} S_{\pi N, \pi N}(E) &= 1 - 2i\pi \frac{\omega_{\pi}(k_{\text{cm}}) \omega_N(k_{\text{cm}})}{E} k_{\text{cm}} T_{\pi N, \pi N}(k_{\text{cm}}, k_{\text{cm}}; E), \\ &= \eta(E) e^{2i\delta(E)}. \end{aligned}$$

- In solving for the energy eigenstates...

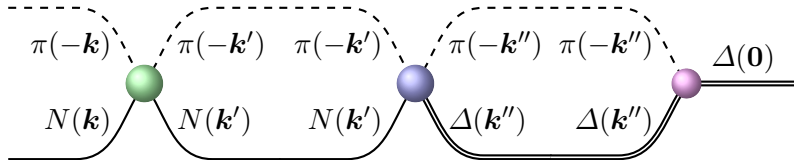


## $\pi N$ phase shift and inelasticity

- The S-matrix is related to the  $T$ -matrix by

$$\begin{aligned} S_{\pi N, \pi N}(E) &= 1 - 2i\pi \frac{\omega_{\pi}(k_{\text{cm}}) \omega_N(k_{\text{cm}})}{E} k_{\text{cm}} T_{\pi N, \pi N}(k_{\text{cm}}, k_{\text{cm}}; E), \\ &= \eta(E) e^{2i\delta(E)}. \end{aligned}$$

- In solving for the energy eigenstates...

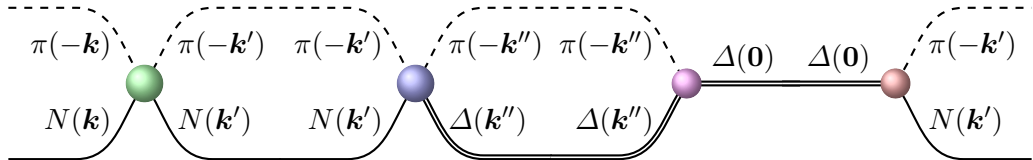


## $\pi N$ phase shift and inelasticity

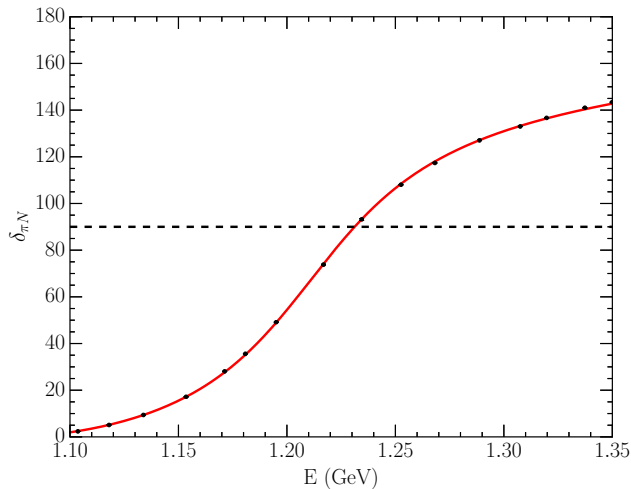
- The S-matrix is related to the  $T$ -matrix by

$$\begin{aligned} S_{\pi N, \pi N}(E) &= 1 - 2i\pi \frac{\omega_\pi(k_{\text{cm}}) \omega_N(k_{\text{cm}})}{E} k_{\text{cm}} T_{\pi N, \pi N}(k_{\text{cm}}, k_{\text{cm}}; E), \\ &= \eta(E) e^{2i\delta(E)}. \end{aligned}$$

- In solving for the energy eigenstates...



# $P$ -wave $\pi N$ phase shifts in the $\Delta$ channel - 1 $\pi N$ channel



## Finite Volume Analysis - Hamiltonian Matrix

- In a finite periodic volume, momentum is quantised to  $n(2\pi/L)$ .

## Finite Volume Analysis - Hamiltonian Matrix

- In a finite periodic volume, momentum is quantised to  $n(2\pi/L)$ .
- In a cubic volume of extent  $L$  on each side, define the momentum magnitudes

$$k_n = \sqrt{n_x^2 + n_y^2 + n_z^2} \frac{2\pi}{L},$$

with  $n_i = 0, 1, 2, \dots$  and integer  $n = n_x^2 + n_y^2 + n_z^2$ .



## Finite Volume Analysis - Hamiltonian Matrix

- In a finite periodic volume, momentum is quantised to  $n(2\pi/L)$ .
- In a cubic volume of extent  $L$  on each side, define the momentum magnitudes

$$k_n = \sqrt{n_x^2 + n_y^2 + n_z^2} \frac{2\pi}{L},$$

with  $n_i = 0, 1, 2, \dots$  and integer  $n = n_x^2 + n_y^2 + n_z^2$ .

- The degeneracy of each  $k_n$  is described by  $C_3(n)$ , which counts the number of ways the integers  $n_x$ ,  $n_y$ , and  $n_z$ , can be squared and summed to  $n$ .

## Finite Volume Analysis - Hamiltonian Matrix

- In a finite periodic volume, momentum is quantised to  $n (2\pi/L)$ .
- In a cubic volume of extent  $L$  on each side, define the momentum magnitudes

$$k_n = \sqrt{n_x^2 + n_y^2 + n_z^2} \frac{2\pi}{L},$$

with  $n_i = 0, 1, 2, \dots$  and integer  $n = n_x^2 + n_y^2 + n_z^2$ .

- The degeneracy of each  $k_n$  is described by  $C_3(n)$ , which counts the number of ways the integers  $n_x$ ,  $n_y$ , and  $n_z$ , can be squared and summed to  $n$ .
- The non-interacting Hamiltonian takes the form

$$H_0 = \text{diag}(m_{B_0}, \omega_{\pi N}(k_0), \omega_{\pi \Delta}(k_0), \omega_{\pi N}(k_1), \omega_{\pi \Delta}(k_1), \dots)$$

## Interaction Hamiltonian Terms

- $1 \rightarrow 2$  particle interaction terms sit in the first row and column.

$$H_I = \begin{pmatrix} 0 & \overline{G}_{\pi N, B_0}(k_0) & \cdots & \overline{G}_{\pi \Delta, B_0}(k_0) & \overline{G}_{\pi N, B_0}(k_1) & \cdots & \overline{G}_{\pi \Delta, B_0}(k_1) \cdots \\ \overline{G}_{\pi N, B_0}^\dagger(k_0) & 0 & & & & & \\ \vdots & & 0 & & & & \\ \overline{G}_{\pi \Delta, B_0}^\dagger(k_0) & & & \ddots & & & \\ \overline{G}_{\pi N, B_0}^\dagger(k_1) & & & & \ddots & & \\ \vdots & & & & & \ddots & \\ \overline{G}_{\pi \Delta, B_0}^\dagger(k_1) & & & & & & \ddots \\ \vdots & & & & & & \end{pmatrix}.$$

- $\dots$  allow for additional channels.

## Interaction Hamiltonian Terms

- $1 \rightarrow 2$  particle interaction terms sit in the first row and column.

$$H_I = \begin{pmatrix} 0 & \overline{G}_{\pi N, B_0}(k_0) & \cdots & \overline{G}_{\pi \Delta, B_0}(k_0) & \overline{G}_{\pi N, B_0}(k_1) & \cdots & \overline{G}_{\pi \Delta, B_0}(k_1) \cdots \\ \overline{G}_{\pi N, B_0}^\dagger(k_0) & 0 & & & & & \\ \vdots & & 0 & & & & \\ \overline{G}_{\pi \Delta, B_0}^\dagger(k_0) & & & \ddots & & & \\ \overline{G}_{\pi N, B_0}^\dagger(k_1) & & & & & & \\ \vdots & & & & & & \\ \overline{G}_{\pi \Delta, B_0}^\dagger(k_1) & & & & & & \\ \vdots & & & & & & \end{pmatrix}.$$

- $\cdots$  allow for additional channels.
- $2 \rightarrow 2$  particle interaction terms,  $\overline{V}_{\alpha, \beta}^S(k_n, k_{n'})$ , fill out the rest of the matrix.

## Relation to infinite-volume contributions

- The finite volume Hamiltonian interaction terms are related to the infinite-volume contributions via

$$\int k^2 dk = \frac{1}{4\pi} \int d^3k \rightarrow \frac{1}{4\pi} \sum_{n \in \mathbb{Z}^3} \left( \frac{2\pi}{L} \right)^3 = \frac{1}{4\pi} \sum_{n \in \mathbb{Z}} C_3(n) \left( \frac{2\pi}{L} \right)^3 .$$

such that

$$\begin{aligned} \bar{G}_{\alpha, B_0}(k_n) &= \sqrt{\frac{C_3(n)}{4\pi}} \left( \frac{2\pi}{L} \right)^{\frac{3}{2}} G_{\alpha, B_0}(k_n) , \\ \bar{V}_{\alpha\beta}^S(k_n, k_m) &= \sqrt{\frac{C_3(n)}{4\pi}} \sqrt{\frac{C_3(m)}{4\pi}} \left( \frac{2\pi}{L} \right)^3 V_{\alpha\beta}^S(k_n, k_m) . \end{aligned}$$

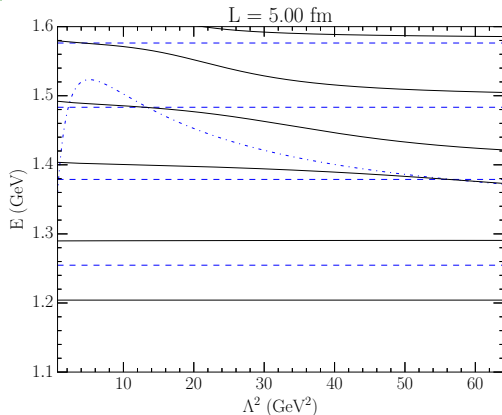
# Finite Volume Eigenmode Solution

- Standard Lapack routines provide eigenmode solutions of

$$\langle i | H | j \rangle \langle j | E_{\alpha} \rangle = E_{\alpha} \langle i | E_{\alpha} \rangle ,$$

- where  $|i\rangle$  and  $|j\rangle$  are the non-interacting basis states,
- $E_{\alpha}$  is the energy eigenvalue, and
- $\langle i | E_{\alpha} \rangle$  is the eigenvector of the
- Hamiltonian matrix  $\langle i | H | j \rangle$ .

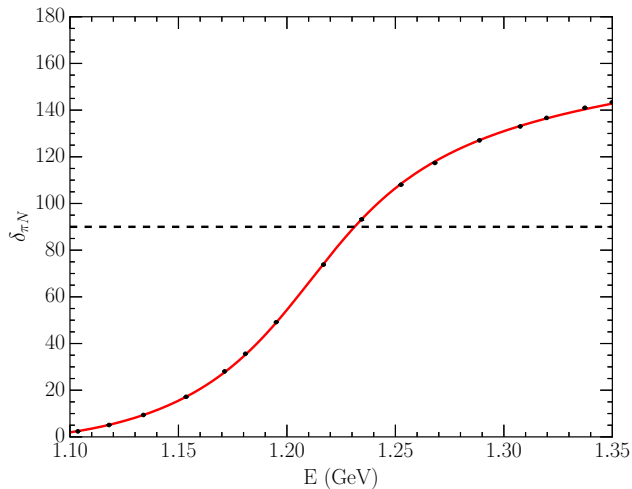
# Energy eigenstates on an $L = 5$ fm lattice for different regulators



- **dashed lines** are the non-interacting  $\pi N$  basis-state energy levels.
- **dot-dash line** is the bare basis-state mass.
- **solid lines** are the eigenstate energy levels.

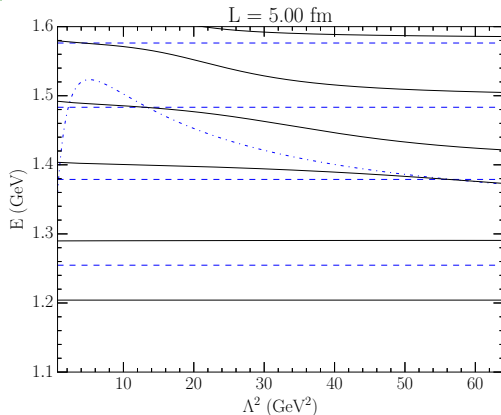
- Incorporation of the Lüscher formalism ensures energy eigenstates below 1.35 GeV are model independent.

# $P$ -wave $\pi N$ phase shifts in the $\Delta$ channel - 1 $\pi N$ channel





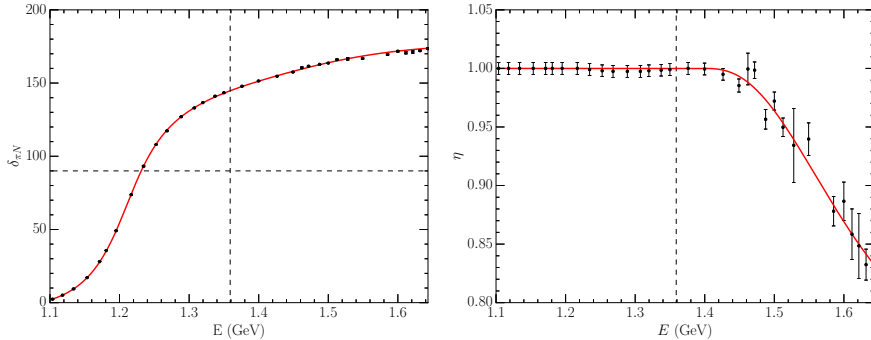
# Energy eigenstates on an $L = 5$ fm lattice for different regulators



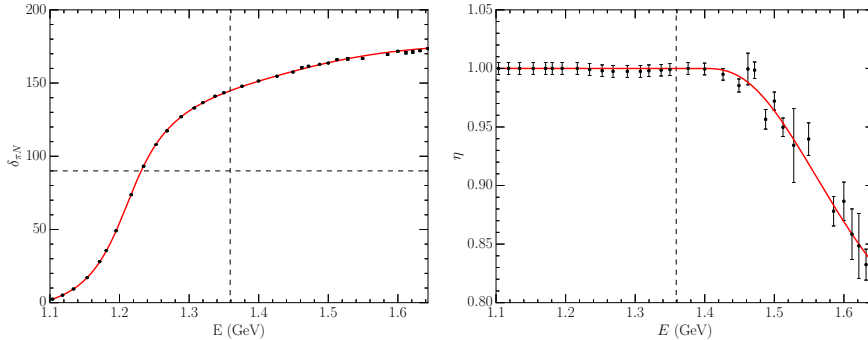
- **dashed lines** are the non-interacting  $\pi N$  basis-state energy levels.
- **dot-dash line** is the bare basis-state mass.
- **solid lines** are the eigenstate energy levels.

- Incorporation of the Lüscher formalism ensures energy eigenstates below 1.35 GeV are model independent.

# $P$ -wave $\pi N$ scattering in the $\Delta$ channel - 2 channel $\pi N$ and $\pi\Delta$

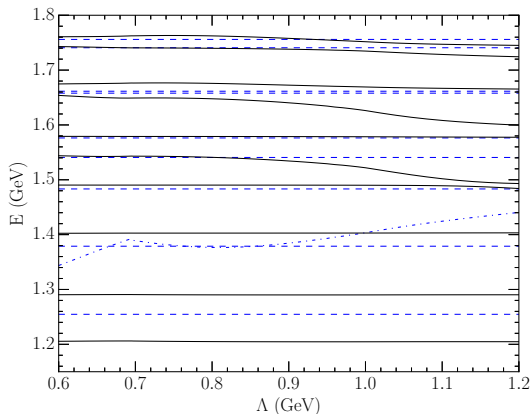


# $P$ -wave $\pi N$ scattering in the $\Delta$ channel - 2 channel $\pi N$ and $\pi\Delta$



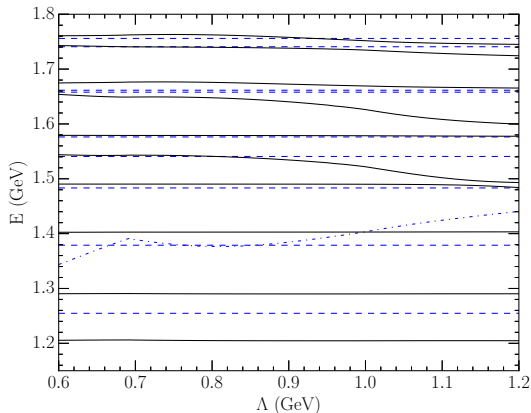
- Anticipate regulator independence to 1.7 GeV.

# Energy eigenstates on an $L = 5$ fm lattice for different regulators



- **dashed lines** are the non-interacting  $\pi N$  and  $\pi \Delta$  basis-state energy levels.
- **dot-dash line** is the bare basis-state mass.
- **solid lines** are the eigenstate energy levels.

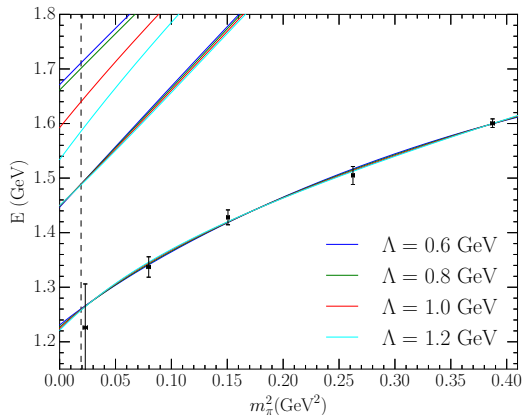
## Energy eigenstates on an $L = 5$ fm lattice for different regulators



- **dashed lines** are the non-interacting  $\pi N$  and  $\pi \Delta$  basis-state energy levels.
- **dot-dash line** is the bare basis-state mass.
- **solid lines** are the eigenstate energy levels.

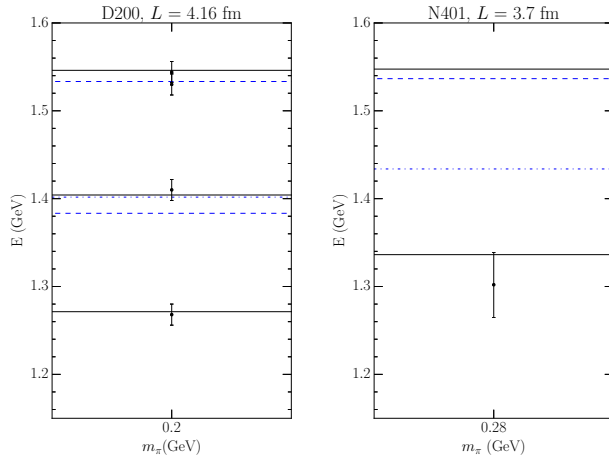
- $\pi N$  scattering data alone is insufficient to uniquely constrain the Hamiltonian.

# Mass dependence of energy eigenstates - Fit to PACS-CS $\Delta$ masses



- Lattice QCD results can constrain the Hamiltonian description of experimental data.

# CLS Consortium finite-volume lattice energies of $\Delta$ -channel excitations



- C. Morningstar, *et al.* PoS **LATTICE2021** (2022), 170 [arXiv:2111.07755 [hep-lat]].
- C. W. Andersen, J. Bulava, B. Hörz and C. Morningstar, Phys. Rev. D **97** (2018) 014506 [arXiv:1710.01557 [hep-lat]].

# New examination of low-lying odd-parity nucleon resonances

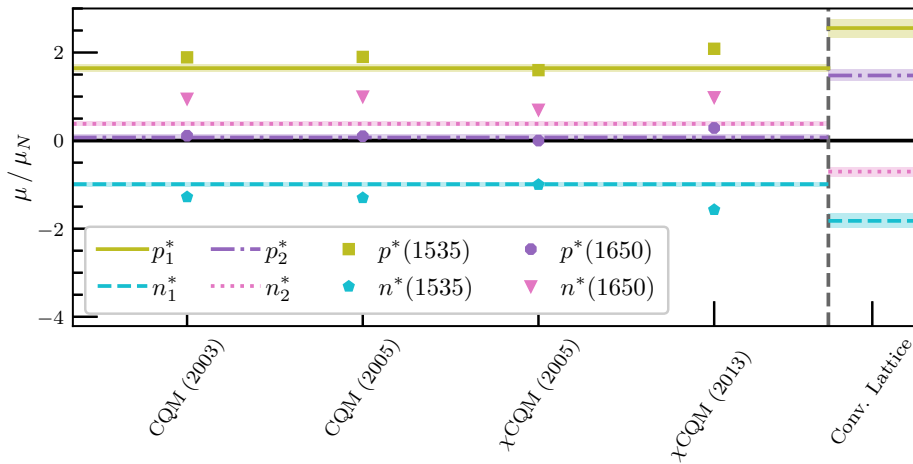
- Motivated by lattice QCD calculations of the electromagnetic form factors of the two low-lying odd-parity states.

F. M. Stokes, W. Kamleh, DBL, Phys. Rev. D **102** (2020) 014507 [arXiv:1907.00177 [hep-lat]].

- Parity-expanded variational analysis (PEVA) removes opposite-parity contaminants.
- Confirms quark model predictions for  $N^*$  magnetic moments.



# $N^*$ Magnetic Moments and the constituent quark model



F. M. Stokes, W. Kamleh, DBL, Phys. Rev. D **102** (2020) 014507 [arXiv:1907.00177 [hep-lat]].

# Model Calculation References

- CQM (2003)

W.-T. Chiang, S. N. Yang, M. Vanderhaeghen, and D. Drechsel, Magnetic dipole moment of the S 11 (1535) from the  $\gamma p \rightarrow \gamma \eta p$  reaction, Nucl. Phys. **A723**, 205 (2003), nucl-th/0211061

- $\chi$ CQM (2005)

J. Liu, J. He, and Y. Dong, Magnetic moments of negative-parity low-lying nucleon resonances in quark models, Phys. Rev. **D71**, 094004 (2005).

- $\chi$ CQM (2013)

N. Sharma, A. Martinez Torres, K. Khemchandani, and H. Dahiya, Magnetic moments of the low-lying  $1/2^-$  octet baryon resonances, Eur. Phys. J. **A49**, 11 (2013), arXiv:1207.3311

## New examination of low-lying odd-parity nucleon resonances

- Both the  $N^*(1535)$  and  $N^*(1650)$  are quark-model like at larger quark masses.

## New examination of low-lying odd-parity nucleon resonances

- Both the  $N^*(1535)$  and  $N^*(1650)$  are quark-model like at larger quark masses.
- Perform the first HEFT analysis with two bare basis states which
  - Mix to form the  $N^*(1535)$  and  $N^*(1650)$ .

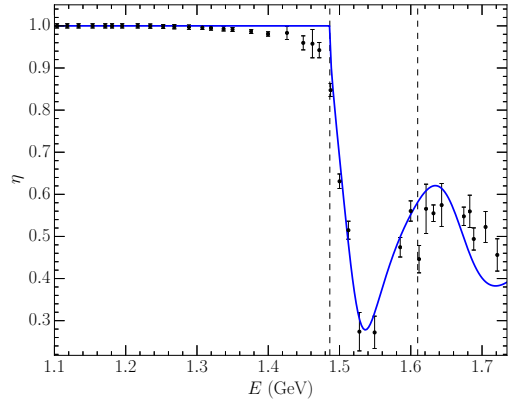
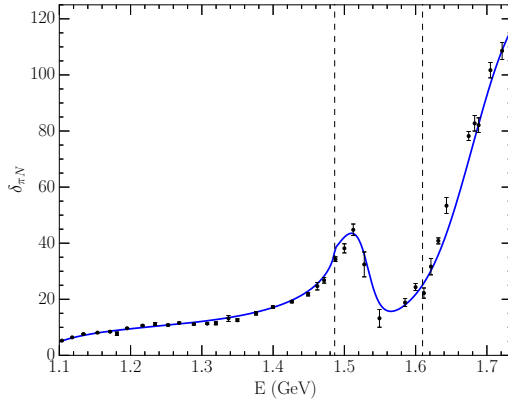
# New examination of low-lying odd-parity nucleon resonances

- Both the  $N^*(1535)$  and  $N^*(1650)$  are quark-model like at larger quark masses.
- Perform the first HEFT analysis with two bare basis states which
  - Mix to form the  $N^*(1535)$  and  $N^*(1650)$ .
- Informed by the decay properties of these resonances and energy thresholds, the calculation includes three meson-baryon scattering channels,  $\pi N$ ,  $\eta N$ , and  $K\Lambda$ .

# New examination of low-lying odd-parity nucleon resonances

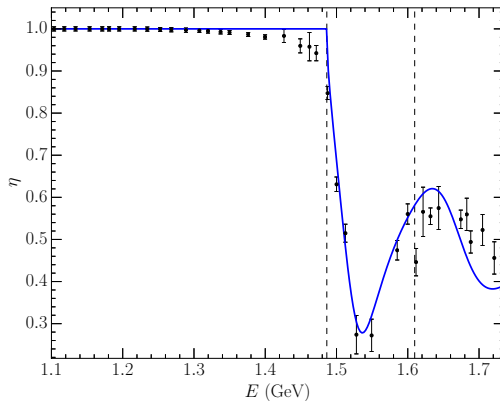
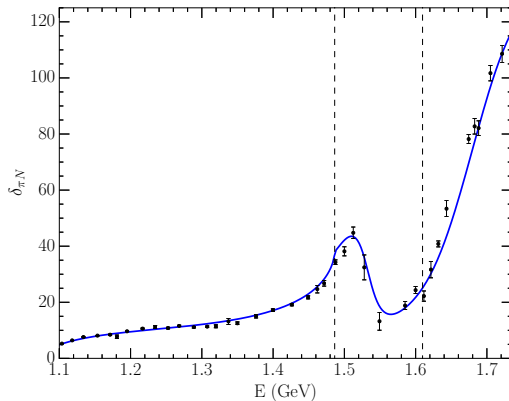
- Both the  $N^*(1535)$  and  $N^*(1650)$  are quark-model like at larger quark masses.
- Perform the first HEFT analysis with two bare basis states which
  - Mix to form the  $N^*(1535)$  and  $N^*(1650)$ .
- Informed by the decay properties of these resonances and energy thresholds, the calculation includes three meson-baryon scattering channels,  $\pi N$ ,  $\eta N$ , and  $K\Lambda$ .
- 21 parameter fit provides an excellent characterisation of the data.
  - Pole positions agree with PDG.

## Phase shift and inelasticity for the low-lying odd-parity spin-1/2 nucleon resonances



- W108 single-energy data from SAID.
- Vertical lines indicate the opening of the  $\eta N$  and  $K\Lambda$  thresholds.

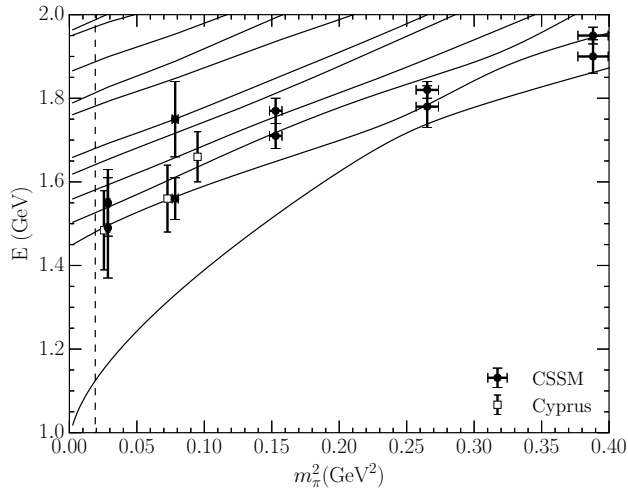
## Phase shift and inelasticity for the low-lying odd-parity spin-1/2 nucleon resonances



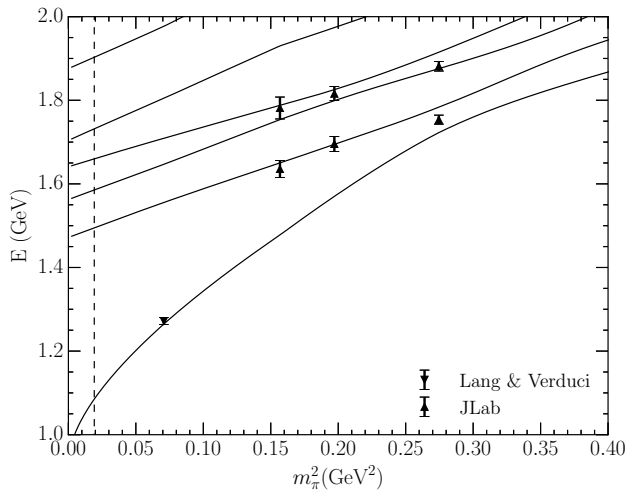
- Note the three-body  $\pi\pi N$  threshold at 1.22 GeV.
- See Max Hansen's talk in Parallel Session 1, today at 4:20 pm.



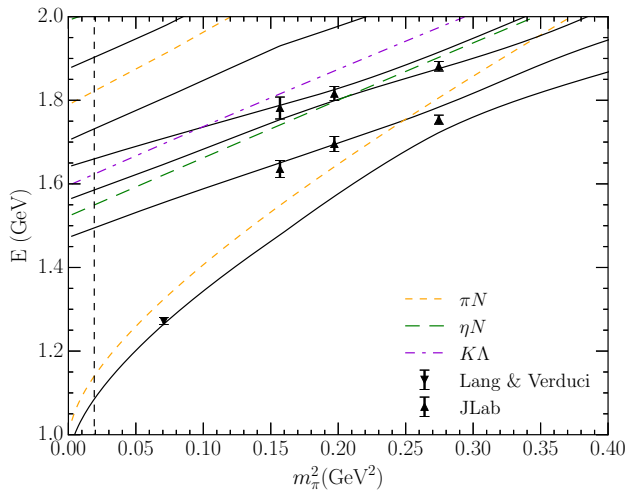
# Finite-volume $L = 3$ fm energy levels for low-lying odd-parity spin-1/2 nucleons



# Finite-volume $L = 2$ fm energy levels for low-lying odd-parity spin-1/2 nucleons



# Finite-volume $L = 2$ fm energy levels for low-lying odd-parity spin-1/2 nucleons



# Finite Volume Eigenmode Solution

- Standard Lapack routines provide eigenmode solutions of

$$\langle i | H | j \rangle \langle j | E_\alpha \rangle = E_\alpha \langle i | E_\alpha \rangle.$$

- Eigenvector  $\langle i | E_\alpha \rangle$  describes the composition of the eigenstate  $| E_\alpha \rangle$  in terms of the basis states  $| i \rangle$  with

$$| i \rangle = | B_0 \rangle, \quad | \pi N, k_0 \rangle, \quad | \pi N, k_1 \rangle, \quad \cdots | \eta N, k_0 \rangle, \quad | \eta N, k_1 \rangle, \quad \cdots.$$

# Finite Volume Eigenmode Solution

- Standard Lapack routines provide eigenmode solutions of

$$\langle i | H | j \rangle \langle j | E_\alpha \rangle = E_\alpha \langle i | E_\alpha \rangle.$$

- Eigenvector  $\langle i | E_\alpha \rangle$  describes the composition of the eigenstate  $| E_\alpha \rangle$  in terms of the basis states  $| i \rangle$  with

$$| i \rangle = | B_0 \rangle, \quad | \pi N, k_0 \rangle, \quad | \pi N, k_1 \rangle, \quad \cdots | \eta N, k_0 \rangle, \quad | \eta N, k_1 \rangle, \quad \cdots.$$

- The overlap of the bare basis state  $| B_0 \rangle$  with eigenstate  $| E_\alpha \rangle$ ,

$$\langle B_0 | E_\alpha \rangle,$$

is of particular interest,

## Finite Volume Eigenmode Solution

- In Hamiltonian EFT, the only localised basis state is the bare basis state.

## Finite Volume Eigenmode Solution

- In Hamiltonian EFT, the only localised basis state is the bare basis state.
- Bär has highlighted how  $\chi$ PT provides an estimate of the direct coupling of smeared nucleon interpolating fields to a non-interacting  $\pi N$  (basis) state,

$$\frac{3}{16} \frac{1}{(f_\pi L)^2 E_\pi L} \left( \frac{E_N - M_N}{E_N} \right) \sim 10^{-3},$$

relative to the ground state.

O. Bar, Phys. Rev. D **92** (2015) no.7, 074504 [arXiv:1503.03649 [hep-lat]].

## Finite Volume Eigenmode Solution

- In Hamiltonian EFT, the only localised basis state is the bare basis state.
- Bär has highlighted how  $\chi$ PT provides an estimate of the direct coupling of smeared nucleon interpolating fields to a non-interacting  $\pi N$  (basis) state,

$$\frac{3}{16} \frac{1}{(f_\pi L)^2 E_\pi L} \left( \frac{E_N - M_N}{E_N} \right) \sim 10^{-3},$$

relative to the ground state.

O. Bar, Phys. Rev. D **92** (2015) no.7, 074504 [arXiv:1503.03649 [hep-lat]].

- Conclude the smeared interpolating fields of lattice QCD are associated with the bare basis states of HEFT

$$\bar{\chi}(0) |\Omega\rangle \simeq |B_0\rangle ,$$



## Finite Volume Eigenmode Solution

- In Hamiltonian EFT, the only localised basis state is the bare basis state.
- Bär has highlighted how  $\chi$ PT provides an estimate of the direct coupling of smeared nucleon interpolating fields to a non-interacting  $\pi N$  (basis) state,

$$\frac{3}{16} \frac{1}{(f_\pi L)^2 E_\pi L} \left( \frac{E_N - M_N}{E_N} \right) \sim 10^{-3},$$

relative to the ground state.

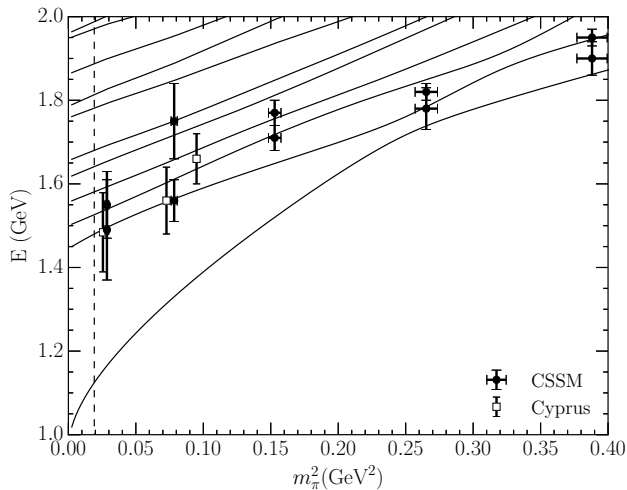
O. Bar, Phys. Rev. D **92** (2015) no.7, 074504 [arXiv:1503.03649 [hep-lat]].

- Conclude the smeared interpolating fields of lattice QCD are associated with the bare basis states of HEFT

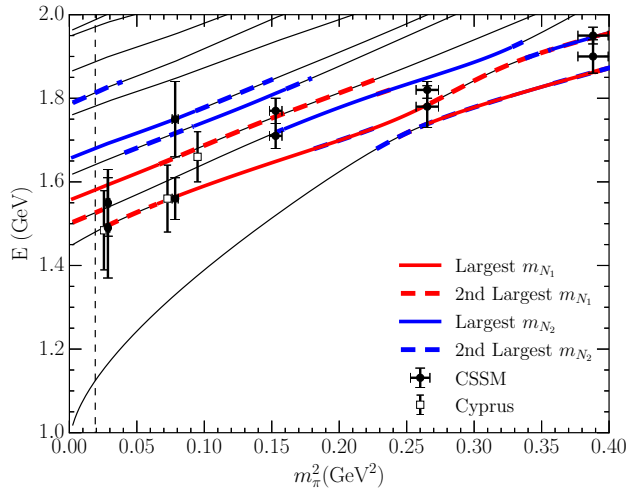
$$\bar{\chi}(0) |\Omega\rangle \simeq |B_0\rangle,$$

- Element  $\langle B_0 | E_\alpha \rangle$  of the eigenvector governs the likelihood of observing  $|E_\alpha\rangle$ .

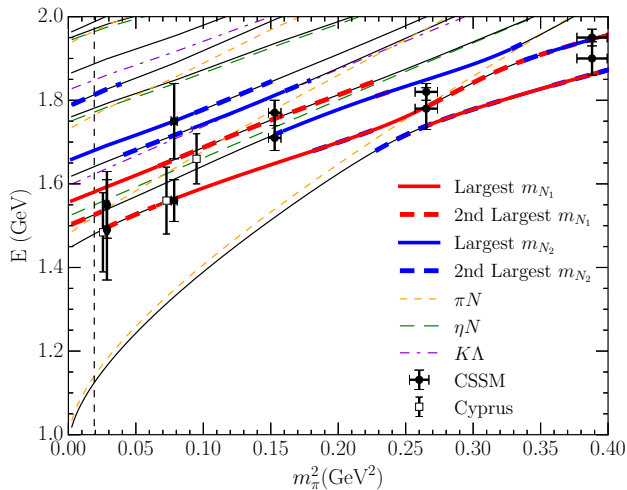
# Finite-volume $L = 3$ fm energy levels for low-lying odd-parity spin-1/2 nucleons



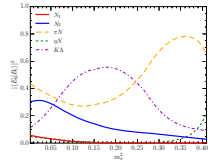
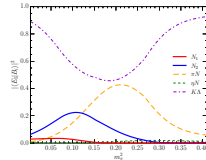
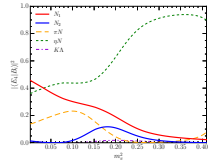
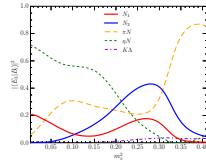
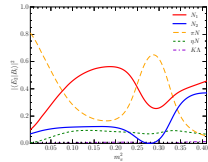
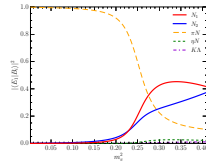
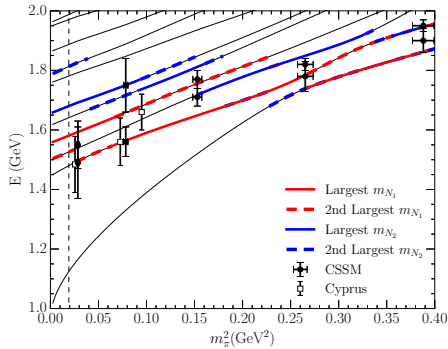
# Finite-volume $L = 3$ fm energy levels for low-lying odd-parity spin-1/2 nucleons



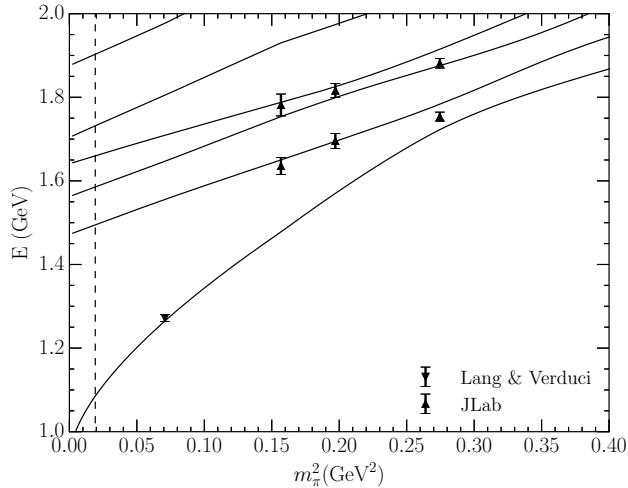
# Finite-volume $L = 3$ fm energy levels for low-lying odd-parity spin-1/2 nucleons



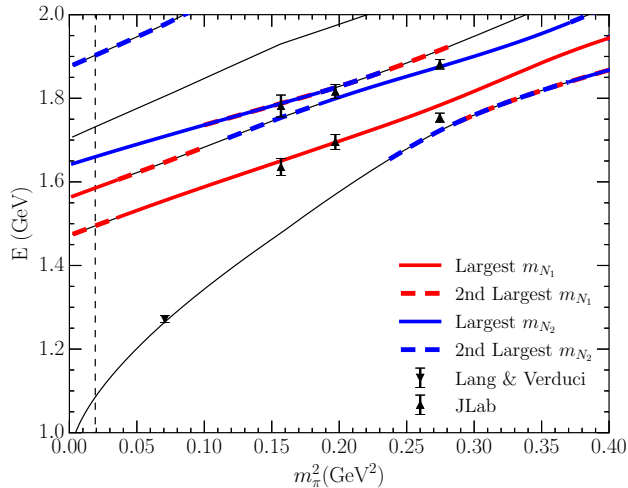
# Energy eigenstate composition - 3 fm lattice



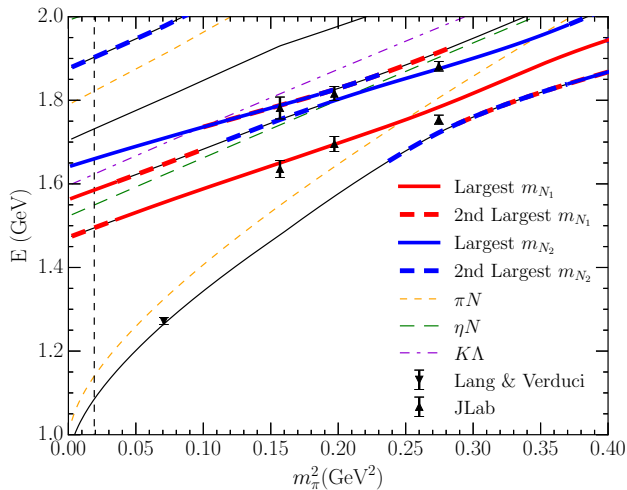
# Finite-volume $L = 2$ fm energy levels for low-lying odd-parity spin-1/2 nucleons



# Finite-volume $L = 2$ fm energy levels for low-lying odd-parity spin-1/2 nucleons

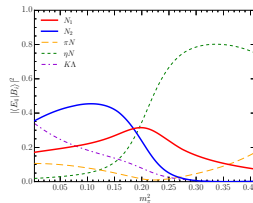
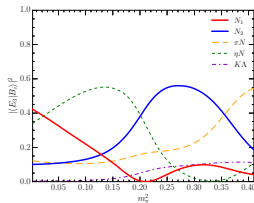
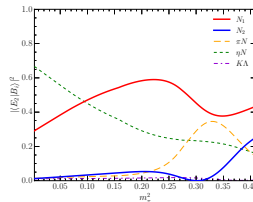
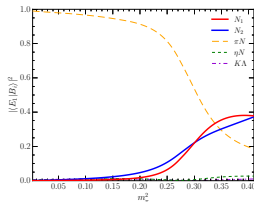
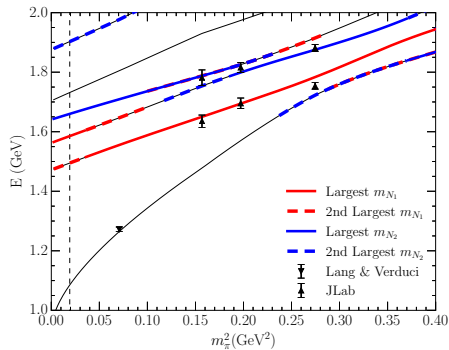


# Finite-volume $L = 2$ fm energy levels for low-lying odd-parity spin-1/2 nucleons





# Energy eigenstate composition - 2 fm lattice



# Analysis of low-lying odd-parity $\Lambda$ resonances

Z. W. Liu, *et al.* [CSSM], Phys. Rev. D **95** (2017) 014506 [arXiv:1607.05856 [nucl-th]]

- Consider  $\pi\Sigma$ ,  $\bar{K}N$ ,  $\eta\Lambda$ ,  $K\Xi$  channels, and one bare basis state,  $B_0$ .

# Analysis of low-lying odd-parity $\Lambda$ resonances

Z. W. Liu, *et al.* [CSSM], Phys. Rev. D **95** (2017) 014506 [arXiv:1607.05856 [nucl-th]]

- Consider  $\pi\Sigma$ ,  $\bar{K}N$ ,  $\eta\Lambda$ ,  $K\Xi$  channels, and one bare basis state,  $B_0$ .
- Eight two-to-two particle couplings are considered for isospin 0 and 1

$$g_{\pi\Sigma,\pi\Sigma}^0, g_{\bar{K}N,\bar{K}N}^0, g_{\bar{K}N,\pi\Sigma}^0, g_H^0, g_{\pi\Sigma,\pi\Sigma}^1, g_{\bar{K}N,\bar{K}N}^1, g_{\bar{K}N,\pi\Sigma}^1, g_{\bar{K}N,\pi\Lambda}^1,$$

# Analysis of low-lying odd-parity $\Lambda$ resonances

Z. W. Liu, *et al.* [CSSM], Phys. Rev. D **95** (2017) 014506 [arXiv:1607.05856 [nucl-th]]

- Consider  $\pi\Sigma$ ,  $\bar{K}N$ ,  $\eta\Lambda$ ,  $K\Xi$  channels, and one bare basis state,  $B_0$ .
- Eight two-to-two particle couplings are considered for isospin 0 and 1

$$g_{\pi\Sigma,\pi\Sigma}^0, g_{\bar{K}N,\bar{K}N}^0, g_{\bar{K}N,\pi\Sigma}^0, g_H^0, g_{\pi\Sigma,\pi\Sigma}^1, g_{\bar{K}N,\bar{K}N}^1, g_{\bar{K}N,\pi\Sigma}^1, g_{\bar{K}N,\pi\Lambda}^1,$$

- Five parameters describing bare to two-particle interactions are introduced

$$m_{B_0}, g_{\pi\Sigma,B_0}^0, g_{\bar{K}N,B_0}^0, g_{\eta\Lambda,B_0}^0, g_{K\Xi,B_0}^0,$$

# Analysis of low-lying odd-parity $\Lambda$ resonances

Z. W. Liu, *et al.* [CSSM], Phys. Rev. D **95** (2017) 014506 [arXiv:1607.05856 [nucl-th]]

- Consider  $\pi\Sigma$ ,  $\bar{K}N$ ,  $\eta\Lambda$ ,  $K\Xi$  channels, and one bare basis state,  $B_0$ .
- Eight two-to-two particle couplings are considered for isospin 0 and 1

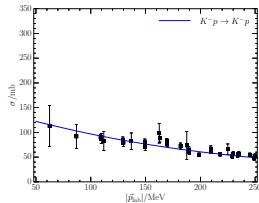
$$g_{\pi\Sigma,\pi\Sigma}^0, g_{\bar{K}N,\bar{K}N}^0, g_{\bar{K}N,\pi\Sigma}^0, g_H^0, g_{\pi\Sigma,\pi\Sigma}^1, g_{\bar{K}N,\bar{K}N}^1, g_{\bar{K}N,\pi\Sigma}^1, g_{\bar{K}N,\pi\Lambda}^1,$$

- Five parameters describing bare to two-particle interactions are introduced

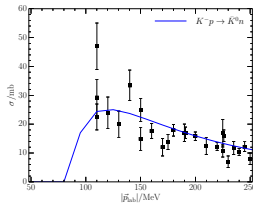
$$m_{B_0}, g_{\pi\Sigma,B_0}^0, g_{\bar{K}N,B_0}^0, g_{\eta\Lambda,B_0}^0, g_{K\Xi,B_0}^0,$$

- These 13 parameters are constrained by experimental data.

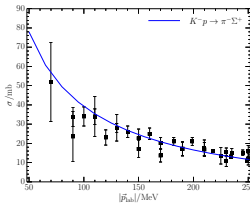
# Couplings and $m_{B_0}$ Constrained by Experiment



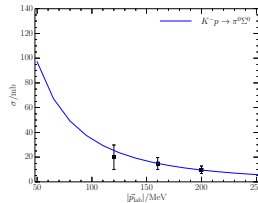
(a)  $K^- p \rightarrow K^- p$



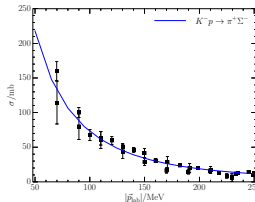
(b)  $K^- p \rightarrow \bar{K}^0 n$



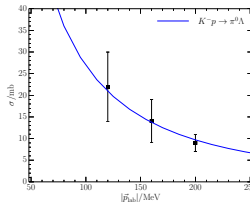
(c)  $K^- p \rightarrow \pi^- \Sigma^+$



(d)  $K^- p \rightarrow \pi^0 \Sigma^0$

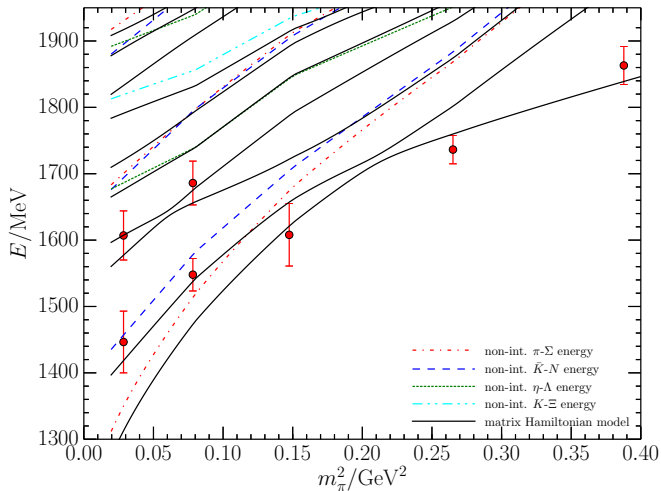


(e)  $K^- p \rightarrow \pi^+ \Sigma^-$

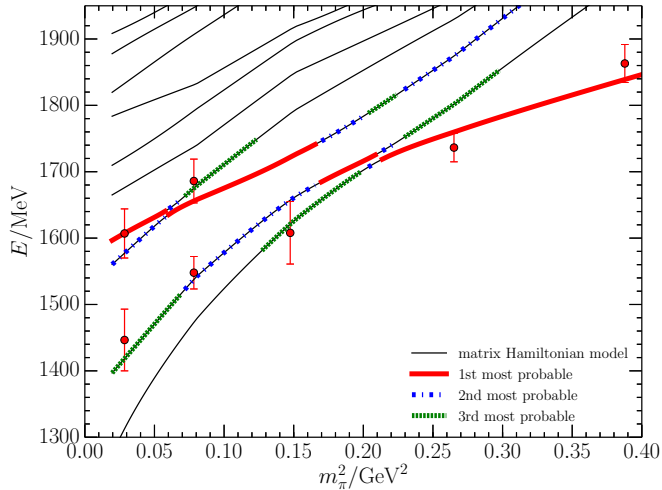


(f)  $K^- p \rightarrow \pi^0 \Lambda$

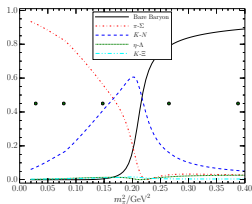
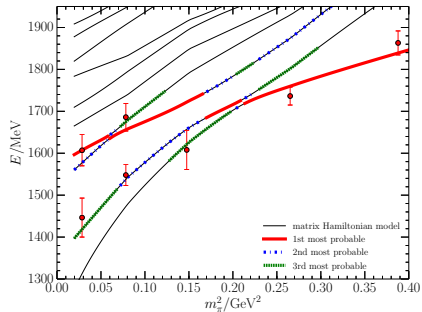
# Finite Volume $\Lambda$ Spectrum for $L = 3$ fm



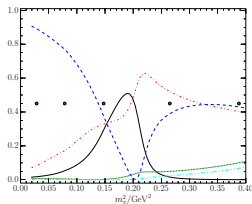
# Finite Volume $\Lambda$ Spectrum for $L = 3$ fm



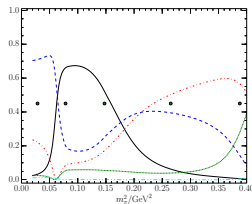




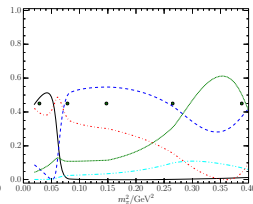
(a) State 1



(b) State 2



(c) State 3



(d) State 4

# Strange Magnetic Form Factor of the $\Lambda(1405)$

J. M. M. Hall, *et al.* [CSSM], Phys. Rev. Lett. **114**, 132002 (2015) arXiv:1411.3402 [hep-lat]

- Provides direct insight into the possible dominance of a molecular  $\bar{K}N$  bound state.

# Strange Magnetic Form Factor of the $\Lambda(1405)$

J. M. M. Hall, *et al.* [CSSM], Phys. Rev. Lett. **114**, 132002 (2015) arXiv:1411.3402 [hep-lat]

- Provides direct insight into the possible dominance of a molecular  $\bar{K}N$  bound state.
- In forming such a molecular state, the  $\Lambda(u, d, s)$  valence quark configuration is complemented by
  - A  $u, \bar{u}$  pair making a  $K^-(s, \bar{u})$  - proton  $(u, u, d)$  bound state, or
  - A  $d, \bar{d}$  pair making a  $\bar{K}^0(s, \bar{d})$  - neutron  $(d, d, u)$  bound state.

# Strange Magnetic Form Factor of the $\Lambda(1405)$

J. M. M. Hall, *et al.* [CSSM], Phys. Rev. Lett. **114**, 132002 (2015) arXiv:1411.3402 [hep-lat]

- Provides direct insight into the possible dominance of a molecular  $\bar{K}N$  bound state.
- In forming such a molecular state, the  $\Lambda(u, d, s)$  valence quark configuration is complemented by
  - A  $u, \bar{u}$  pair making a  $K^-(s, \bar{u})$  - proton  $(u, u, d)$  bound state, or
  - A  $d, \bar{d}$  pair making a  $\bar{K}^0(s, \bar{d})$  - neutron  $(d, d, u)$  bound state.
- In both cases the strange quark is confined within a spin-0 kaon and has no preferred spin orientation.

# Strange Magnetic Form Factor of the $\Lambda(1405)$

J. M. M. Hall, *et al.* [CSSM], Phys. Rev. Lett. **114**, 132002 (2015) arXiv:1411.3402 [hep-lat]

- Provides direct insight into the possible dominance of a molecular  $\bar{K}N$  bound state.
- In forming such a molecular state, the  $\Lambda(u, d, s)$  valence quark configuration is complemented by
  - A  $u, \bar{u}$  pair making a  $K^-(s, \bar{u})$  - proton  $(u, u, d)$  bound state, or
  - A  $d, \bar{d}$  pair making a  $\bar{K}^0(s, \bar{d})$  - neutron  $(d, d, u)$  bound state.
- In both cases the strange quark is confined within a spin-0 kaon and has no preferred spin orientation.
- To conserve parity, the kaon has zero orbital angular momentum.

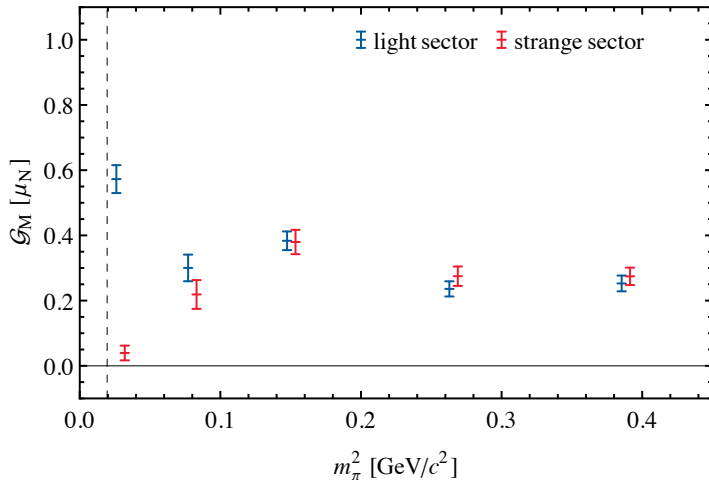
## Strange Magnetic Form Factor of the $\Lambda(1405)$

J. M. M. Hall, *et al.* [CSSM], Phys. Rev. Lett. **114**, 132002 (2015) arXiv:1411.3402 [hep-lat]

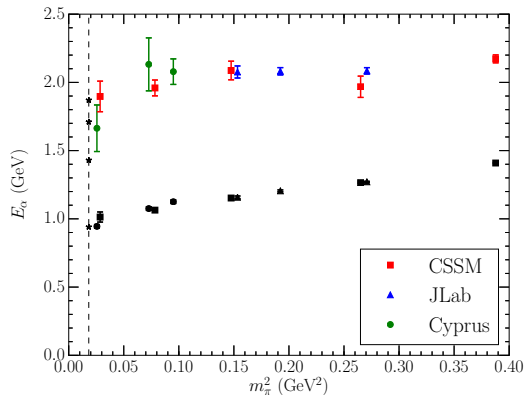
- Provides direct insight into the possible dominance of a molecular  $\bar{K}N$  bound state.
- In forming such a molecular state, the  $\Lambda(u, d, s)$  valence quark configuration is complemented by
  - A  $u, \bar{u}$  pair making a  $K^-(s, \bar{u})$  - proton  $(u, u, d)$  bound state, or
  - A  $d, \bar{d}$  pair making a  $\bar{K}^0(s, \bar{d})$  - neutron  $(d, d, u)$  bound state.
- In both cases the strange quark is confined within a spin-0 kaon and has no preferred spin orientation.
- To conserve parity, the kaon has zero orbital angular momentum.
- Thus, the strange quark does not contribute to the magnetic form factor of the  $\Lambda(1405)$  when it is dominated by a  $\bar{K}N$  molecule.

# Strange Magnetic Form Factor of the $\Lambda(1405)$

J. M. M. Hall, *et al.* [CSSM], Phys. Rev. Lett. **114**, 132002 (2015) arXiv:1411.3402 [hep-lat]



# Where is the Roper resonance?

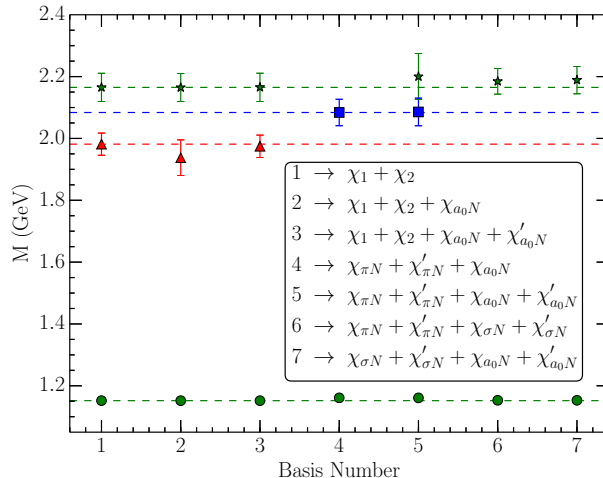


- CSSM: Z. W. Liu, *et al.* [CSSM], Phys. Rev. D **95**, 034034 (2017) arXiv:1607.04536 [nucl-th]
- Cyprus: C. Alexandrou, *et al.* (AMIAS), Phys. Rev. D **91**, 014506 (2015) arXiv:1411.6765 [hep-lat]
- JLab: R. G. Edwards, *et al.* [HSC] Phys. Rev. D **84**, 074508 (2011) [arXiv:1104.5152 [hep-ph]].

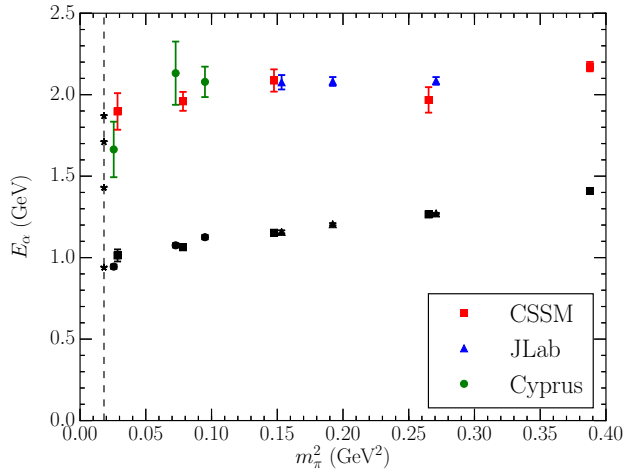


# Search for low-lying lattice QCD eigenstates in the Roper regime

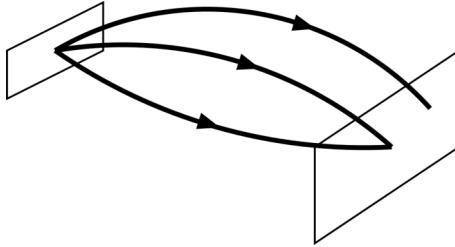
A. L. Kiratidis, *et al.*, [CSSM] Phys. Rev. D **95**, no. 7, 074507 (2017) [arXiv:1608.03051 [hep-lat]].



# Have we seen the $2s$ excitation of the quark model?

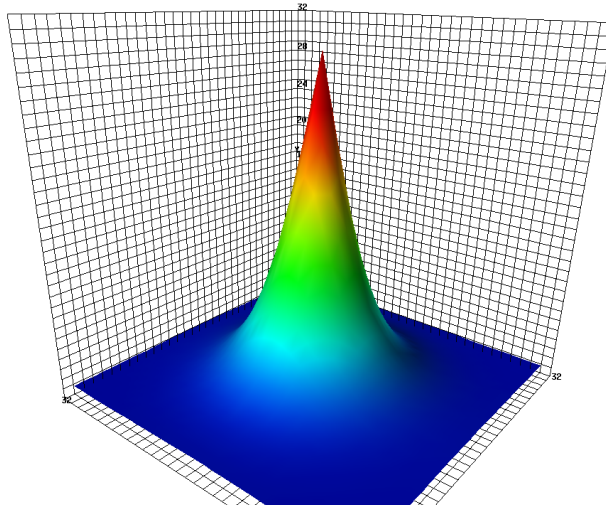


# Landau-Gauge Wave functions from the Lattice

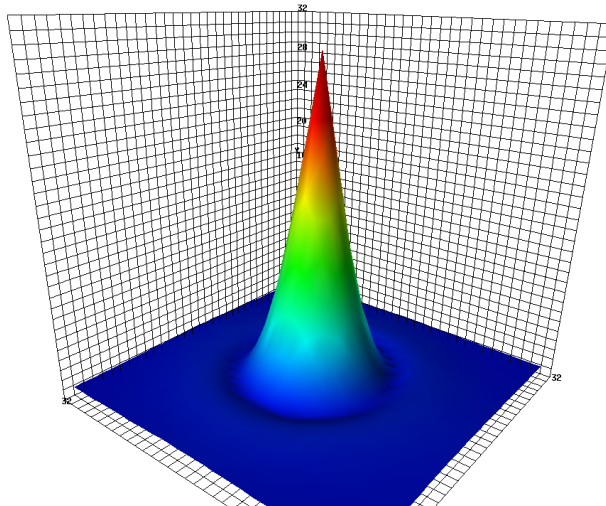


- Measure the *overlap* of the annihilation operator with the state as a function of the quark positions.

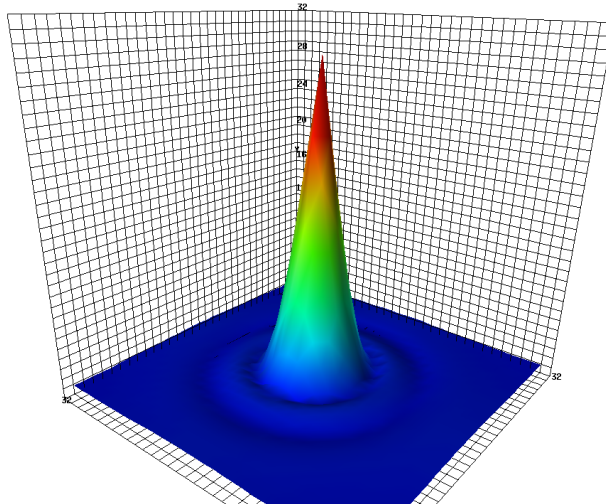
# $d$ -quark probability density in ground state proton [CSSM]



# $d$ -quark probability density in 1st excited state of proton [CSSM]

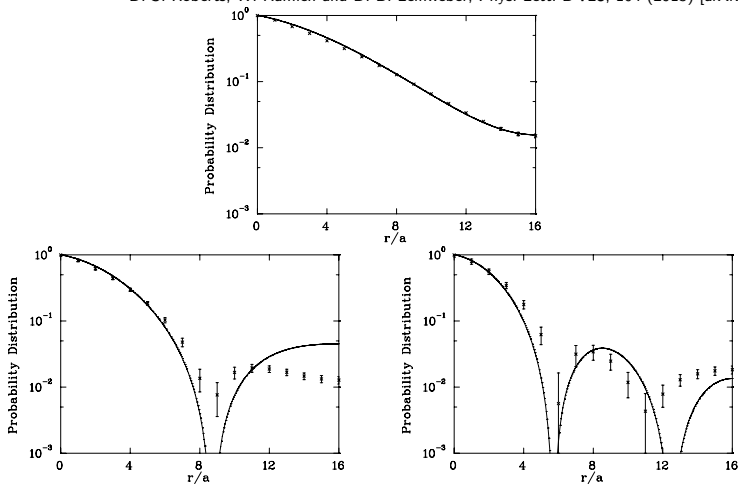


# $d$ -quark probability density in $N = 3$ excited state of proton [CSSM]

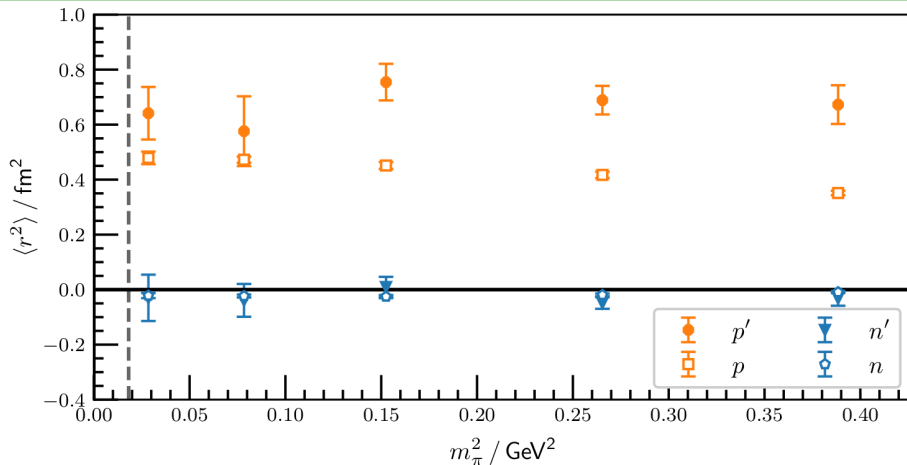


# Comparison with the Simple Quark Model [CSSM]

D. S. Roberts, W. Kamleh and D. B. Leinweber, Phys. Lett. B **725**, 164 (2013) [arXiv:1304.0325 [hep-lat]].



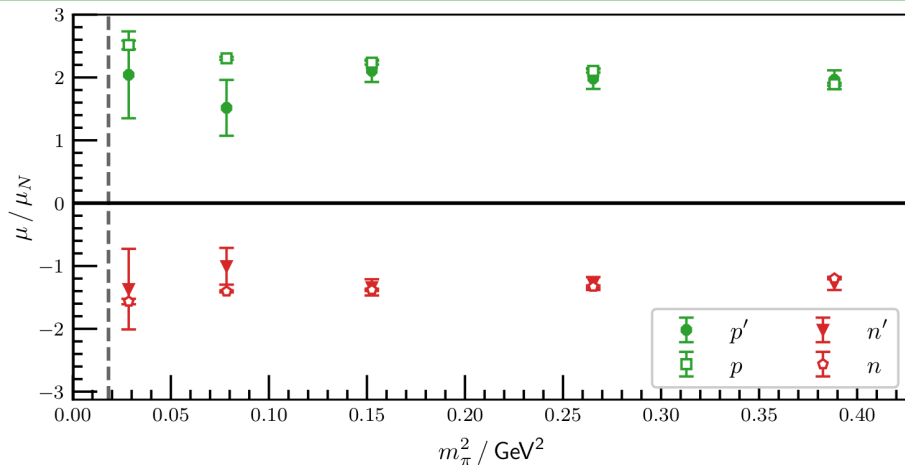
# First positive-parity excitation: Charge Radii



F. M. Stokes, W. Kamleh, DBL, Phys. Rev. D **102** (2020) 014507 [arXiv:1907.00177 [hep-lat]].

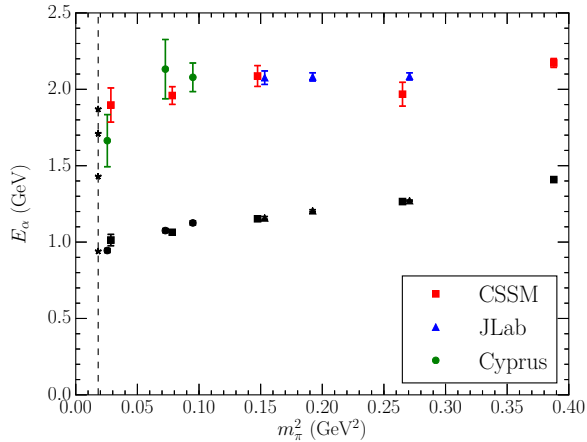


# First positive-parity excitation: Magnetic moments

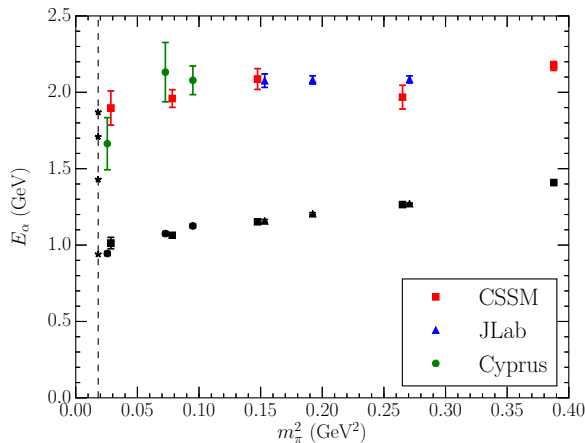


F. M. Stokes, W. Kamleh, DBL, Phys. Rev. D **102** (2020) 014507 [arXiv:1907.00177 [hep-lat]].

# The $2s$ excitation of the nucleon sits at 1.9 GeV

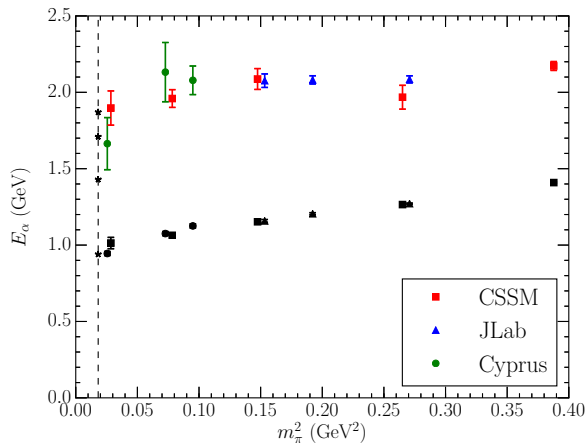


# The $2s$ excitation of the nucleon sits at 1.9 GeV



- The  $N1/2^+(1880)$  observed in photoproduction is associated with the  $2s$  excitation of the nucleon.
- Z. W. Liu, W. Kamleh, DBL, F. M. Stokes, A. W. Thomas and J. J. Wu, Phys. Rev. D **95**, no. 3, 034034 (2017) [arXiv:1607.04536 [nucl-th]]

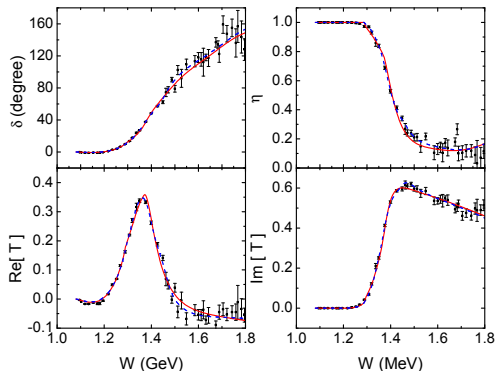
# The $2s$ excitation of the nucleon sits at 1.9 GeV



- The  $N1/2^+(1880)$  observed in photoproduction is associated with the  $2s$  excitation of the nucleon.
- Z. W. Liu, W. Kamleh, DBL, F. M. Stokes, A. W. Thomas and J. J. Wu, Phys. Rev. D **95**, no. 3, 034034 (2017) [arXiv:1607.04536 [nucl-th]]
- What about the Roper resonance?

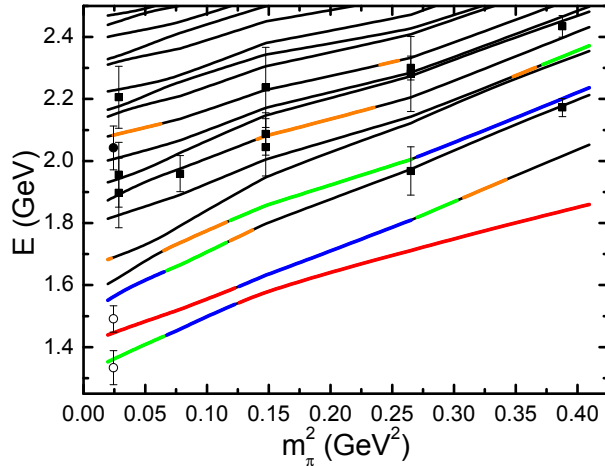
## Positive-parity Nucleon Spectrum: Bare Roper Case with $m_0 = 1.7$ GeV

- Consider  $\pi N$ ,  $\pi\Delta$  and  $\sigma N$  channels, dressing a bare state.
- Fit to phase shift and inelasticity. (dashed blue curve)



- Fit yields two poles in the region of the PDG estimate  $1365 \pm 15 - i 95 \pm 15$  MeV.

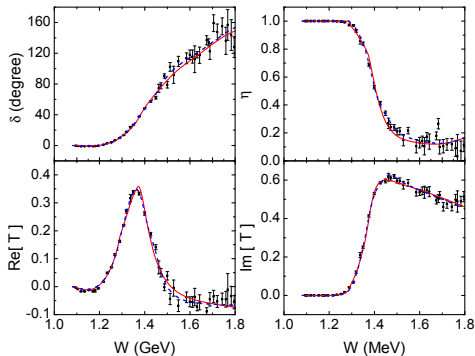
# 1.7 GeV Bare Roper: Hamiltonian Model $N'$ Spectrum



# Positive-parity Nucleon Spectrum: Bare Roper Case with $m_0 = 2.0$ GeV

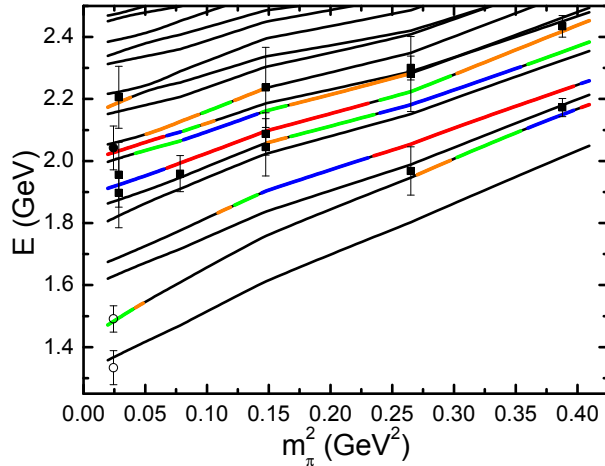
J. j. Wu, et al. [CSSM], arXiv:1703.10715 [nucl-th]

- Consider  $\pi N$ ,  $\pi\Delta$  and  $\sigma N$  channels, dressing a bare state.
- Fit to phase shift and inelasticity. (red curve)



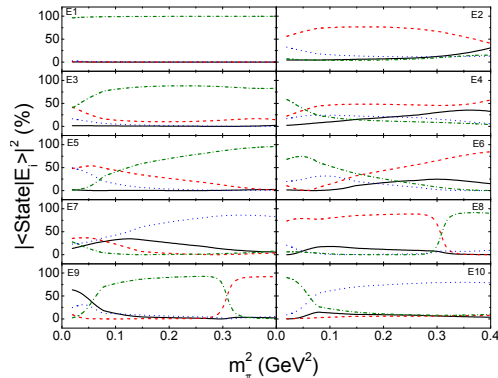
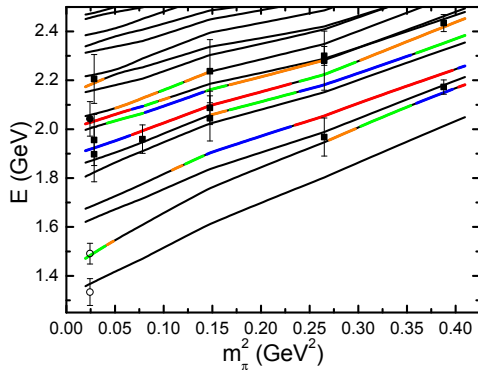
- Fit yields a pole at  $1393 - i 167$  MeV  $\sim$  PDG estimate  $1365 \pm 15 - i 95 \pm 15$  MeV.

## 2.0 GeV Bare Roper: Hamiltonian Model $N'$ Spectrum





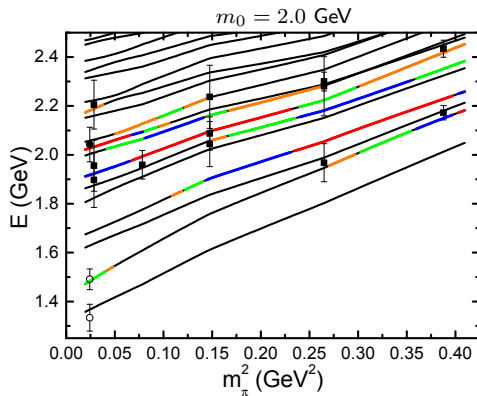
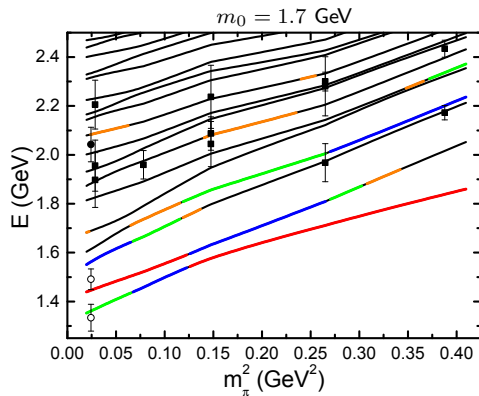
## 2.0 GeV Bare Roper: Hamiltonian Model $N'$ Spectrum



$\pi N$ ,  $\pi \Delta$  and  $\sigma N$  channels, dressing a bare state.

C. B. Lang, L. Leskovec, M. Padmanath and S. Prelovsek, Phys. Rev. D **95**, no. 1, 014510 (2017) [arXiv:1610.01422 [hep-lat]].

## Two different descriptions of the Roper resonance



(left) Meson dressings of a quark-model like core.

(right) Resonance generated by strong rescattering in meson-baryon channels.

## Score Card

Criteria

$m_0 = 1.7 \text{ GeV}$     $m_0 = 2.0 \text{ GeV}$

Describes experimental data well.

## Score Card

Criteria	$m_0 = 1.7 \text{ GeV}$	$m_0 = 2.0 \text{ GeV}$
Describes experimental data well.	✓	✓

## Score Card

Criteria	$m_0 = 1.7 \text{ GeV}$	$m_0 = 2.0 \text{ GeV}$
Describes experimental data well.	✓	✓
Produces poles in accord with PDG.		

## Score Card

Criteria	$m_0 = 1.7 \text{ GeV}$	$m_0 = 2.0 \text{ GeV}$
Describes experimental data well.	✓	✓
Produces poles in accord with PDG.	✓	✓

## Score Card

Criteria	$m_0 = 1.7 \text{ GeV}$	$m_0 = 2.0 \text{ GeV}$
Describes experimental data well.	✓	✓
Produces poles in accord with PDG.	✓	✓
1st lattice scattering state created via $\sigma N$ interpolator has dominant $\langle \sigma N   E_1 \rangle$ in HEFT.		

# Score Card

Criteria	$m_0 = 1.7 \text{ GeV}$	$m_0 = 2.0 \text{ GeV}$
Describes experimental data well.	✓	✓
Produces poles in accord with PDG.	✓	✓
1st lattice scattering state created via $\sigma N$ interpolator has dominant $\langle \sigma N   E_1 \rangle$ in HEFT.	✓	✓



## Score Card

Criteria	$m_0 = 1.7 \text{ GeV}$	$m_0 = 2.0 \text{ GeV}$
Describes experimental data well.	✓	✓
Produces poles in accord with PDG.	✓	✓
1st lattice scattering state created via $\sigma N$ interpolator has dominant $\langle \sigma N   E_1 \rangle$ in HEFT.	✓	✓
2nd lattice scattering state created via $\pi N$ interpolator has dominant $\langle \pi N   E_2 \rangle$ in HEFT.		

## Score Card

Criteria	$m_0 = 1.7 \text{ GeV}$	$m_0 = 2.0 \text{ GeV}$
Describes experimental data well.	✓	✓
Produces poles in accord with PDG.	✓	✓
1st lattice scattering state created via $\sigma N$ interpolator has dominant $\langle \sigma N   E_1 \rangle$ in HEFT.	✓	✓
2nd lattice scattering state created via $\pi N$ interpolator has dominant $\langle \pi N   E_2 \rangle$ in HEFT.	✗	✓

## Score Card

Criteria	$m_0 = 1.7 \text{ GeV}$	$m_0 = 2.0 \text{ GeV}$
Describes experimental data well.	✓	✓
Produces poles in accord with PDG.	✓	✓
1st lattice scattering state created via $\sigma N$ interpolator has dominant $\langle \sigma N   E_1 \rangle$ in HEFT.	✓	✓
2nd lattice scattering state created via $\pi N$ interpolator has dominant $\langle \pi N   E_2 \rangle$ in HEFT.	✗	✓
L-QCD states excited with 3-quark ops. are associated with HEFT states with large $\langle B_0   E_\alpha \rangle$ .		

# Score Card

Criteria	$m_0 = 1.7 \text{ GeV}$	$m_0 = 2.0 \text{ GeV}$
Describes experimental data well.	✓	✓
Produces poles in accord with PDG.	✓	✓
1st lattice scattering state created via $\sigma N$ interpolator has dominant $\langle \sigma N   E_1 \rangle$ in HEFT.	✓	✓
2nd lattice scattering state created via $\pi N$ interpolator has dominant $\langle \pi N   E_2 \rangle$ in HEFT.	✗	✓
L-QCD states excited with 3-quark ops. are associated with HEFT states with large $\langle B_0   E_\alpha \rangle$ .	✗	✓

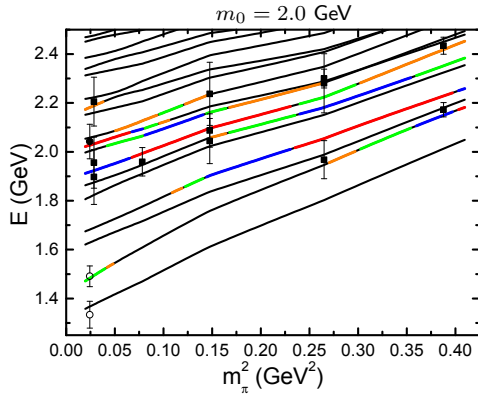
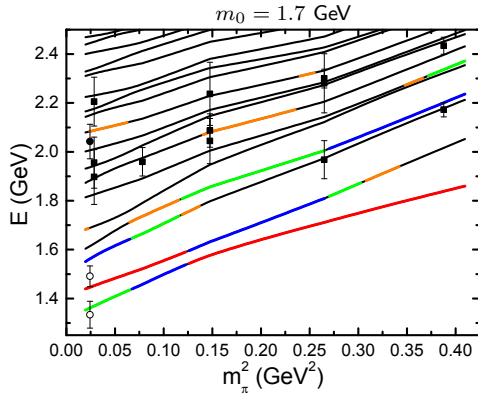
# Score Card

Criteria	$m_0 = 1.7 \text{ GeV}$	$m_0 = 2.0 \text{ GeV}$
Describes experimental data well.	✓	✓
Produces poles in accord with PDG.	✓	✓
1st lattice scattering state created via $\sigma N$ interpolator has dominant $\langle \sigma N   E_1 \rangle$ in HEFT.	✓	✓
2nd lattice scattering state created via $\pi N$ interpolator has dominant $\langle \pi N   E_2 \rangle$ in HEFT.	✗	✓
L-QCD states excited with 3-quark ops. are associated with HEFT states with large $\langle B_0   E_\alpha \rangle$ .	✗	✓
HEFT predicts three-quark states that exist in lattice QCD.		

# Score Card

Criteria	$m_0 = 1.7 \text{ GeV}$	$m_0 = 2.0 \text{ GeV}$
Describes experimental data well.	✓	✓
Produces poles in accord with PDG.	✓	✓
1st lattice scattering state created via $\sigma N$ interpolator has dominant $\langle \sigma N   E_1 \rangle$ in HEFT.	✓	✓
2nd lattice scattering state created via $\pi N$ interpolator has dominant $\langle \pi N   E_2 \rangle$ in HEFT.	✗	✓
L-QCD states excited with 3-quark ops. are associated with HEFT states with large $\langle B_0   E_\alpha \rangle$ .	✗	✓
HEFT predicts three-quark states that exist in lattice QCD.	✗	✓

## Two different descriptions of the Roper resonance



(left) Meson dressings of a quark-model like core.

(right) Resonance generated by strong rescattering in meson-baryon channels.

## Conclusion

---

- The Roper resonance is not associated with a low-lying three-quark core.



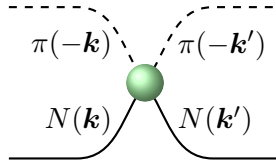
## Conclusion

---

- The Roper resonance is not associated with a low-lying three-quark core.
- The Roper resonance is generated by strong rescattering in meson-baryon channels.

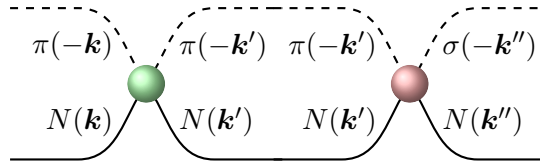
# Conclusion

- The Roper resonance is not associated with a low-lying three-quark core.
- The Roper resonance is generated by strong rescattering in meson-baryon channels.



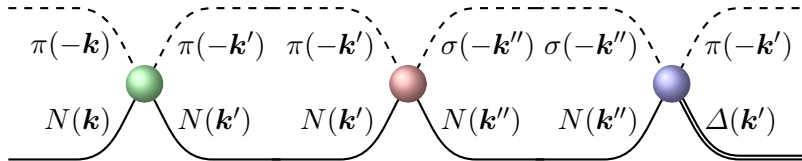
## Conclusion

- The Roper resonance is not associated with a low-lying three-quark core.
- The Roper resonance is generated by strong rescattering in meson-baryon channels.



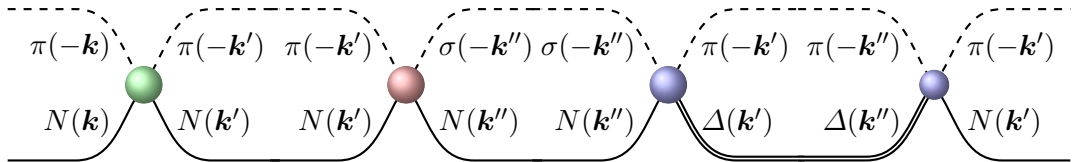
## Conclusion

- The Roper resonance is not associated with a low-lying three-quark core.
- The Roper resonance is generated by strong rescattering in meson-baryon channels.



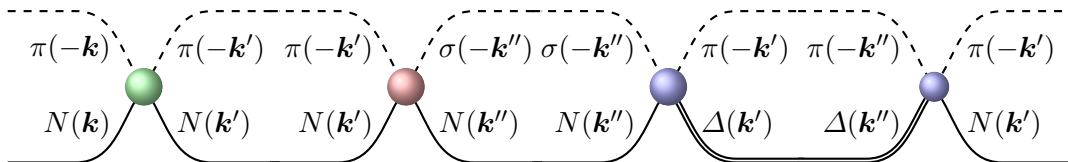
## Conclusion

- The Roper resonance is not associated with a low-lying three-quark core.
- The Roper resonance is generated by strong rescattering in meson-baryon channels.



## Conclusion

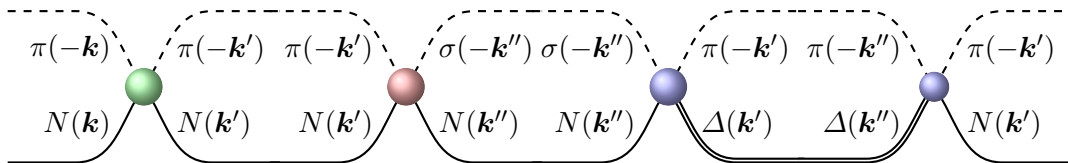
- The Roper resonance is not associated with a low-lying three-quark core.
- The Roper resonance is generated by strong rescattering in meson-baryon channels.



- The  $2s$  excitation of the nucleon is dressed to lie at  $\sim 1.9$  GeV

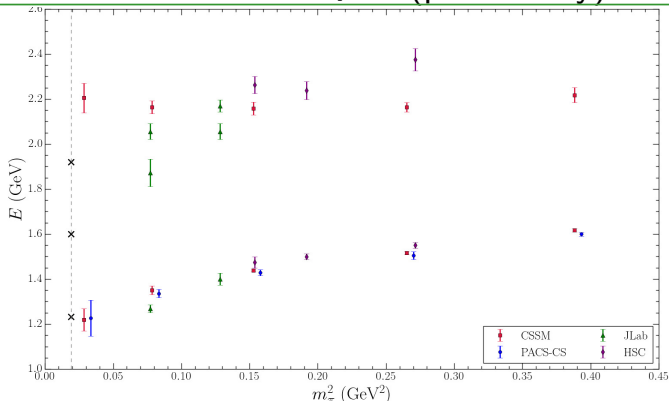
## Conclusion

- The Roper resonance is not associated with a low-lying three-quark core.
- The Roper resonance is generated by strong rescattering in meson-baryon channels.



- The  $2s$  excitation of the nucleon is dressed to lie at  $\sim 1.9$  GeV
- The lattice state in the Roper region has  $\sim 5\%$  bare state contribution.

# $\Delta$ -baryon spectrum from lattice QCD (preliminary)



**HSC:** J. Bulava, *et al.*, Phys. Rev. D **82** (2010) 014507 [arXiv:1004.5072 [hep-lat]].

**JLab:** T. Khan, D. Richards and F. Winter, Phys. Rev. D **104** (2021) 034503 [arXiv:2010.03052 [hep-lat]].

**PACS-CS:** S. Aoki *et al.* [PACS-CS], Phys. Rev. D **79** (2009) 034503 [arXiv:0807.1661 [hep-lat]].



## Conclusions

---

- Hamiltonian Effective Field Theory (HEFT)
  - Connects infinite-volume scattering observables to finite-volume Lattice QCD.

## Conclusions

---

- Hamiltonian Effective Field Theory (HEFT)
  - Connects infinite-volume scattering observables to finite-volume Lattice QCD.
  - Connects lattice results at different quark masses within a single formalism.

# Conclusions

---

- Hamiltonian Effective Field Theory (HEFT)
  - Connects infinite-volume scattering observables to finite-volume Lattice QCD.
  - Connects lattice results at different quark masses within a single formalism.
  - Provides insight into the composition of energy eigenstates.
  - Facilitates an understanding of lattice QCD results.

# Conclusions

---

- Hamiltonian Effective Field Theory (HEFT)
  - Connects infinite-volume scattering observables to finite-volume Lattice QCD.
  - Connects lattice results at different quark masses within a single formalism.
  - Provides insight into the composition of energy eigenstates.
  - Facilitates an understanding of lattice QCD results.
  - With lattice QCD constraints, HEFT provides new insight into resonance structure.

# Conclusions

- Hamiltonian Effective Field Theory (HEFT)
  - Connects infinite-volume scattering observables to finite-volume Lattice QCD.
  - Connects lattice results at different quark masses within a single formalism.
  - Provides insight into the composition of energy eigenstates.
  - Facilitates an understanding of lattice QCD results.
  - With lattice QCD constraints, HEFT provides new insight into resonance structure.
- $\Delta$  Resonance: illustrate Lüscher constraints and the role of lattice QCD constraints.

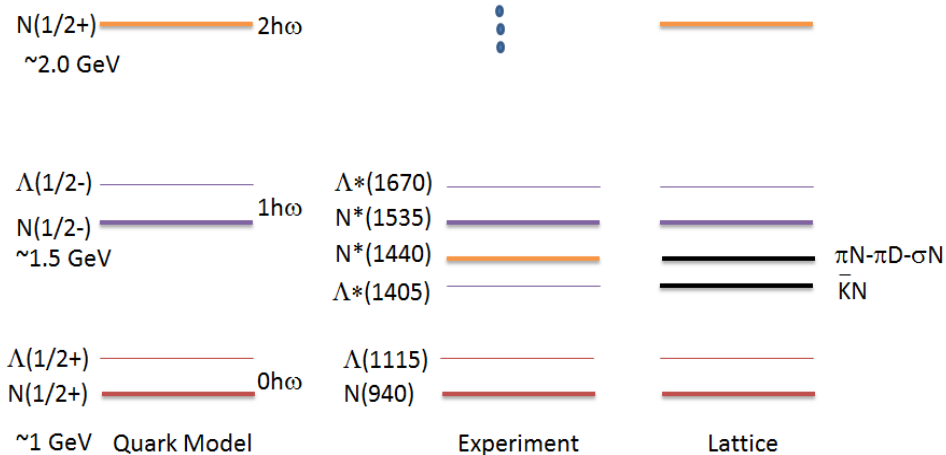
## Conclusions

- Hamiltonian Effective Field Theory (HEFT)
  - Connects infinite-volume scattering observables to finite-volume Lattice QCD.
  - Connects lattice results at different quark masses within a single formalism.
  - Provides insight into the composition of energy eigenstates.
  - Facilitates an understanding of lattice QCD results.
  - With lattice QCD constraints, HEFT provides new insight into resonance structure.
- $\Delta$  Resonance: illustrate Lüscher constraints and the role of lattice QCD constraints.
- Odd-parity  $N^*(1535)$  and  $N^*(1650)$  Resonances:
  - Knowledge of eigenstate composition can be used to understand the states observed.
  - Dominated by a quark-core bare state dressed by meson degrees of freedom.

# Conclusions

- Hamiltonian Effective Field Theory (HEFT)
  - Connects infinite-volume scattering observables to finite-volume Lattice QCD.
  - Connects lattice results at different quark masses within a single formalism.
  - Provides insight into the composition of energy eigenstates.
  - Facilitates an understanding of lattice QCD results.
  - With lattice QCD constraints, HEFT provides new insight into resonance structure.
- $\Delta$  Resonance: illustrate Lüscher constraints and the role of lattice QCD constraints.
- Odd-parity  $N^*(1535)$  and  $N^*(1650)$  Resonances:
  - Knowledge of eigenstate composition can be used to understand the states observed.
  - Dominated by a quark-core bare state dressed by meson degrees of freedom.
- Roper  $N(1440)$  Resonance: Arises from dynamical coupled-channel effects.
  - Lattice QCD results constrain the HEFT description of experimental data.
  - State composition matches when the  $2s$  excitation of the quark model sits at  $\sim 2$  GeV.

# The spectrum of quark-model-like states is relatively simple





# HEFT Extensions

- Formalism for partial-wave mixing in HEFT has been developed in Y. Li, J. J. Wu, C. D. Abell, D. B. L. and A. W. Thomas. Phys. Rev. D **101**, no.11, 114501 (2020) [arXiv:1910.04973 [hep-lat]]
- And extended to moving and elongated finite-volumes in Y. Li, J. J. Wu, D. B. L. and A. W. Thomas Phys. Rev. D **103** no.9, 094518 (2021) [arXiv:2103.12260 [hep-lat]].